British Journal of Pharmacology. Accepted Version 2017: DOI: 10.1111/bph.13889

Big conductance calcium-activated potassium channel openers control spasticity without sedation

David Baker[1,2*], Gareth Pryce[1,2*], Cristina Visintin[2,3], Sofia Sisay[1], Alexander I. Bondarenko[4,5], W.S. Vanessa Ho[6], Samuel J. Jackson[1], Thomas E. Williams[1], Sarah Al-Izki[1], Ioanna Sevastou[3], Masahiro Okuyama[3], Wolfgang F. Graier[4], Lesley A. Stevenson[6], Carolyn. Tanner[7], Ruth Ross[7], Roger G. Pertwee[7], Christopher M. Henstridge[8], Andrew J. Irving[8], Jesse Schulman[9], Keith Powell[9], Mark D. Baker[1], Gavin Giovannoni[1,2] and David L. Selwood[3*]

[1.] Neuroimmunology Unit, Blizard Institute, Barts and the London School of Medicine and Dentistry, Queen Mary University of London, E1 2AT, United Kingdom

[2.] Department of Neuroinflammation, UCL Institute of Neurology, University College London, London WC1N 3BG, UK.

[3.] Department of Medicinal Chemistry, UCL Wolfson Institute for Biomedical Research, University College London, London WC1E 6BT, UK.

[4.] Institute of Molecular Biology and Biochemistry, Medical University of Graz, A-8010, Austria.

[5]. A.A. Bogomoletz Institute of Physiology, Kiev 01024, Ukraine.

[6.] Vascular Biology Research Centre. St. George's, University of London, SW17 ORE, UK.

[7.] Department of Biomedical Sciences, Institute of Medical Sciences, University of Aberdeen, Aberdeen AB25 2ZD, UK.

[8.] Neurosciences Institute, Division of Pathology and Neuroscience, Ninewells Hospital and Medical School, University of Dundee, Dundee, DD1 9SY, UK.

[9.] Canbex Therapeutics Ltd, London BioScience Innovation Centre, London NW1 0NH, UK.

*These authors contributed equally to the work

Running title: BK_{Ca} channels control spasticity

Correspondence: Prof. David Baker. Neuroimmunology Unit, Blizard Institute, Barts and the London School of Medicine and Dentistry, Queen Mary University of London, 4 Newark Street, Whitechapel, London E1 4AT, United Kingdom. Email: david.baker@qmul.ac.uk, Tel: +44(0)20 7882 2485, Fax: +44(0)20 7882 2180.

ABSTRACT

Background & Purpose: The initial aim was to generate cannabinoid agents that control spasticity, occurring as a consequence of multiple sclerosis, whilst avoiding the sedative, side-effect-potential associated with cannabis. (R,Z)-3-(6-(dimethylamino)-6-oxohex-1-enyl)-N-(1-hydroxypropan-2-yl)benzamide (VSN16R) was synthesized as an anandamide (endocannabinoid) analogue in an anti-metabolite approach to identify drug-like agents to target spasticity.

Experimental Approach: Following the initial chemistry, a variety of biochemical, pharmacological and electrophysiological approaches, using isolated cells, tissue-based assays and *in vivo* animal models, were used to demonstrate: activity, efficacy, pharmacokinetics and mechanism of action of the molecule. Toxicological and safety studies in animals and humans demonstrated tolerability of the molecule.

Key Results: VSN16R had nanomolar activity in tissue-based, functional assays and dose-dependently inhibited spasticity in a mouse experimental encephalomyelitis model of multiple sclerosis. This occurred with over a thousand-fold therapeutic window, without affecting normal muscle tone. Efficacy was achieved at plasma levels that were easily achievable and safe in humans. Interestingly, VSN16R did not bind to known CB1/CB2/GPPR55 cannabinoid-related receptors in receptor-based assays, but was found to act on a vascular cannabinoid target. This was identified to be the major neuronal form of the big conductance, calcium-activated potassium (BK_{Ca}) channel. Drug-induced opening of neuronal BK_{Ca} channels induced membrane hyperpolarization to limit excessive neural-excitability and control spasticity.

Conclusions and Implications: This study identifies a novel role of BK_{Ca} channels, a novel mechanism to control spasticity and identifies a new, safe and selective type of ligand to control neural hyper-excitability in spasticity and a number of other neurological conditions.

ABBREVIATIONS

BK_{Ca}	big conductance calcium-activated potassium channel
CB_1R	cannabinoid receptor one
C_{max}	maximum concentration
T_{max}	Time of C_{max}
EAE	experimental autoimmune encephalomyelitis
FPKM	fragments per kilobase of exon per million fragments mapped
MS	multiple sclerosis
SAD	single ascending dose

INTRODUCTION

Multiple sclerosis (MS) is the major cause of non-traumatic disability in young adults. Disease induces neurological attacks and nerve damage leading to impaired neurotransmission and the development of a number of poorly-controlled, troublesome symptoms (Compston & Coles 2002). Spasticity is a common major debilitating consequence of MS (Barnes et al. 2003) and is clinically defined as a velocity-dependent increase in muscle tone resulting from hyper-excitable stretch reflexes, spasms and hypersensitivity to normally innocuous sensory stimulations (Trompetto et al. 2014). The intermittent or sustained involuntary muscle hyperactivity that characterises spasticity is associated with upper motor neuron lesions that can be located anywhere along the path of the corticospinal (pyramidal) tracts from the brain to the spinal cord (Baker et al. 2012, Trompetto et al. 2014). Whilst the aetiology of spasticity in MS has been relatively little studied, this contrasts to experimental spasticity caused by spinal cord injury, where persistent inward sodium and calcium currents and changes in chloride ion balance in motor neurons and increases in the number of primary afferent projections to the motor nerves are believed to be key mechanisms mediating spasticity (Li et al. 2004, Trompetto et al. 2014, Toda et al. 2014). Clinically, these are currently treated using either nerve blocking procedures or pharmacological agents such as depolarizing-ion channel inhibitors; $GABA_A$ and $GABA_B$ receptor agonists; alpha2 adrenergic receptor agonists; dantrolene within the muscle, and more recently nabiximols (medical cannabis) to target the CB_1 cannabinoid receptor (CB_1R) within in the periphery and the CNS (Baker et al. 2000, Shakespeare et al. 2003, Novotna et al. 2011, Baker et al. 2012, Pryce et al. 2014). Whilst these pharmacological treatments are active, their use is associated with dose-limiting side-effects that limit compliance and early adoption following the development of spasticity. (Shakespeare et al. 2003, Novotna et al. 2011, Baker et al. 2012).

We have established a relapsing progressive experimental autoimmune encephalomyelitis (EAE) model of MS in ABH mice as a system for the study of spasticity (Baker et al. 2000, Baker et al. 2012). This model responds to standard spasticity therapies (Baker et al. 2012, Hillard et al. 2012) and was utilized to provide the initial experimental demonstration that cannabis and the endocannabinoid system could control spasticity (Baker et al. 2012, Hillard et al. 2012). The endocannabinoid signalling pathway is part of a much wider lipid signalling system with pleiotropic actions in the CNS, cardiovascular and immune systems (Howlett et al. 2002). Anandamide is one of the key endogenous endocannabinoid mediators and a close analogue, methanandamide can inhibit spasticity in EAE (Baker et al. 2000). As anandamide is rapidly degraded *in vivo* (Howlett et al. 2002), an anti-metabolite approach to create a more stable, drug-like molecule with a good potential to interfere with cannabinoid signalling and avoid brain-mediated side-effects, we synthesised a series of monocyclic alkyl amides (Hoi et al. 2007), based on constrained conformations of anandamide (Berglund et al. 2000; Supplementary Data. Figure S1). We show here that

one compound 3-(6-(dimethylamino)-6-oxohex-1-enyl)-N-(1-hydroxypropan-2-yl)benzamide, (VSN16. Hoi et al. 2007), has potent activity in tissue-based cannabinoid receptor assays, yet was active in CB_1-R deficient mice, pointing to a new target. We identify the neuronal form of the large conductance calcium-activated potassium channel (BK_{Ca}) as the target for VSN16 and demonstrate that activation alleviates neuronal excitability and spasticity in an experimental model of MS.

METHODS

Animals. Adult Biozzi male and female ABH mice were from stock bred either at the Institute of Neurology (ION) or Queen Mary University of London (QMUL) or were purchased from Harlan UK (Bicester, UK). Congenic-ABH CB_1R (Pryce et al. 2003) or G-protein 55 receptor (GPR55)-deficient mice (Sisay et al. 2013) were from stock bred either at ION or QMUL. Outbred mice and rats were purchased from Charles Rivers (Margate, UK) or Harlan Olac (Oxford UK). Animal work was performed following ethical review by the Local Animal Welfare and Ethical Review Bodies and the UK Government Home Office. Animal experiments were performed under the Animals (Scientific Procedures) Act 1986 and European Union Directives 86/609/EEC and EU 2010/63/EU. Animal housing and other elements related to documenting protocols of *in vivo* experiments under the ARRIVE guidelines and experimental design requirements (Curtis et al. 2015), have been reported previously (Al-Izki et al. 2012).

Humans. Healthy volunteers were enrolled in a double-blind, placebo-controlled Phase I safety study, (EudraCT 2013-002765-18) following ethical review of the project (Office of Research Ethics Northern Ireland) and informed consent that complied with the Declaration of Helsinki, GCP (CPMP/ICH/135/95) and local regulation. At the time of designing the study, reproductive toxicity had not been completed. Therefore for safety reasons and ease of recruitment, only males were studied. Individuals were screened negative for amphetamine, ecstasy, benzodiazepines, ethanol, methadone metabolites, cannabinoids, barbiturates, cocaine, urine creatinine, opiates, cotinine and tricyclic anti-depressants. Individuals were randomized to receive either 25mg, 50mg, 100mg, 200mg, 400mg or 800mg (n=six/group) formulated VSN16R or placebo capsules (n=two/group) as part of single ascending dose study of multiple ascending dose study with twice a day 25mg, 100mg and 400mg VSN16R for one week (n=six/group). A randomization schedule was provided to the pharmacist, but study personnel were blinded to this. These people were fasted before dosing, except one group that were fed a standardized high fat breakfast within 0.5h prior to dosing (n=six). Serial plasma samples using EDTA anti-coagulant, were collected. This study was performed by Quintiles Limited London, UK. The sample size was based on experience from previous similar Phase 1 studies with other compounds to obtain adequate safety, tolerability, and

pharmacokinetics data to achieve the objectives of the study while limiting exposing few subjects to drug and procedures.

Chemicals. The production and synthesis of VSN16 (318Da) and the VSN16R and VSN16S enantiomers and VSN22 has been described previously (Hoi et al. 2007). VSN44 was synthesized (Supplementary data. Methods S1). These compounds were additionally synthesized to either Good Manufacturing Practice or Good Laboratories Practice Standards by Sygnature Chemical Services (Nottingham, UK), Park Place Research (Cardiff, UK) or Dalton Chemical Laboratories Inc. (Toronto, Canada). VSN16R for human use was formulated in 25mg and 100mg gelatin capsules by Dalton Chemical Laboratories. R(+)WIN55-212 was purchased from Tocris Ltd. (Bristol, UK) and ± Baclofen was purchased from Sigma Aldrich Ltd (Poole, UK). 1′, 1′-dimethylheptyl-M8-tetrahydrocannabinol-11-oic acid (CT3) was supplied by Atlantic Ventures Inc. (New York, USA) (Pryce et al. 2014). BMS-204352; NS-1619, NS-11021, paxilline and CNQX were purchased from Tocris Ltd or Sigma (Poole UK). Compounds were dissolved in water; saline or DMSO (WIN55) or ethanol prior to dilution with cremaphor (Sigma) and phosphate buffered saline (PBS. 1:1:18). These were delivered via the oral; intra-peritoneal or intravenous routes at less than 5mL/kg, typically 0.1mL in mice and 0.5mL in rats. Although VSN16R is water soluble (>30mg/mL), for high concentrations (200mg/mL) VSN16R was dissolved in 20% polypropylene in water.

Toxicology. Twenty-eight day toxicology in rats and dogs for Investigational New Drug filing was performed by Charles Rivers (UK). Reproductive toxicology in rabbits was performed by Charles Rivers (Canada). Pharmacokinetic and/or toxicological doses ranged from 5-1000mg/kg p.o. in Sprague Dawley male and female rats (n=six-twenty-six/group), 50-200mg/kg p.o. in male and female Beagle dogs (n=six/group) and 100-750mg/kg p.o. in female New Zealand white rabbits (n=nine/group). Results are expressed as mean ± SD. The sample size was based on experience from previous similar toxicology studies with other compounds to obtain adequate safety, tolerability, and pharmacokinetics data to achieve the objectives of the study.

Electrically-evoked contraction of the mouse vas deferens. Vasa deferentia were obtained from outbred MF-1 mice and mounted vertically in a 4mL organ bath at an initial tension of 0.5 g. The baths contained Mg^{2+}-free Krebs solution (NaCl 118.2mM, KCl 4.75mM, KH_2PO_4 1.19mM, $NaHCO_3$ 25.0mM, glucose 11.0mM and $CaCl_2 \cdot 6H_2O$ 2.54mM), which was kept at 35-36 °C and bubbled with 95% O_2 and 5% CO_2. Isometric contractions were evoked by stimulation with 0.5s trains of three pulses of 110% maximal voltage (train frequency 0.1 Hz; pulse duration 0.5 ms) through a platinum electrode attached to the upper end and a stainless steel electrode attached to the lower end of each bath (Ross et al. 2001). Contractions

were monitored by computer using a data recording and analysis system as described previously (Ross et al. 2001). After placement in an organ bath, each tissue was subjected to a stimulation-free period of 10 min and then stimulated for 10 min. Tissues were then subjected to alternate periods of stimulation (5 min) and rest (10 min) until consistent twitch amplitudes were obtained. This equilibration procedure was followed by a stimulation-free period of 25 min. Tissues were then stimulated for 5 min after which the first agonist addition was made and stimulation continued until the end of the experiment.

Receptor Binding. Receptor binding/agonism activity of 10µM VSN16R, plus positive controls, was performed of cell lines transfected with human cannabinoid *CNR1* and *CNR2* and large number of other receptors and transporters and was performed by Cerep SA, (Poitiers, France); Chantest Inc. (Cleveland Ohio), DiscoveRx (Birmingham, UK); Multispan Inc., (Hayward, CA, USA) and MDS Pharma services (Taipei, Taiwan).

Methoxamine-evoked contraction of rat mesenteric artery. Adult male Wistar rats (200-350g) were killed by cervical dislocation and the third-order branches of the superior mesenteric artery, which provides blood supply to the intestine, were removed and cleaned of adherent tissue. Segments (2 mm in length) were mounted in a Mulvany-Halpern type wire myograph (Model 610M; Danish Myo Technology, Aarhus, Denmark) and maintained at 37ºC in gassed (95% O_2/5% CO_2) Krebs-Henseleit solution of the following composition (mM): 118mM NaCl, 4.7mM KCl, 1.2mM $MgSO_4$, 1.2mM KH_2PO4, 25mM $NaHCO_3$, 2mM $CaCl_2$ and 10mM D-glucose 10, as previously described (Ho & Randall 2007). Vessels were equilibrated and set to a basal tension of 2 to 2.5 mN. The integrity of the endothelium was assessed by precontracting the vessel with 10 µM methoxamine (an α_1-adrenoceptor agonist), followed by relaxation with 10 µM carbachol (a muscarinic acetylcholine receptor agonist); vessels showing relaxations of greater than 90% were designated as endothelium-intact. When endothelium was not required, it was removed by rubbing the intima with a human hair; carbachol-induced relaxation of less than 10% indicated successful removal. After the test for endothelial integrity, vessels were left for 30 min and then pre-contracted with 10 µM methoxamine. This was followed by construction of a cumulative concentration-relaxation curve to VSN16R (10nM-1 µM). To investigate the relaxation mechanisms of VSN16R, calcium-activated, potassium channel blockers (apamin, charybdotoxin or iberiotoxin) were incubated with the vessels either alone or in combination before construction of the concentration-response curves to VSN16R. The tension generated by methoxamine in control vessels was 9.4 ± 0.6 mN, as compared with 10.4 ± 2.5 mN in endothelium-denuded vessels, or 10.5 ± 0.5 mN in the presence of calcium-activated, potassium channel inhibitors. Most experiments were performed in matched vessels; effects of blockers or endothelial removal were compared with the control responses obtained in separate vessels of the same rats. All relaxant

responses are expressed as percentage relaxation of the tone induced by methoxamine. Values are given as mean ± SEM. Statistical comparisons of concentration-dependent responses were made by two way analysis of variance (ANOVA) using Prism 4 (GraphPad Software, Inc, San Diego, CA, USA).

Patch clamp of calcium-activated potassium channels recording in human cells. The human EA.hy926 endothelial cells (ATCC, Manassas, USA) and were grown in DMEM containing 10% FCS and 1% HAT (5 mM hypoxanthin, 20 μM aminopterin, 0.8 mM thymidine) and were maintained in an incubator at 37°C in 5% CO_2 atmosphere (Bondarenko et al. 2013). Human HNC-2 neuronal cells were obtained from ATCC. For experiments, cells were plated on glass coverslips. Single-channel recordings were obtained from excised inside-out membrane patches in symmetrical solutions using the patch-clamp technique. All patch-clamp experiments were performed at room temperature with the use of a water hydraulic micromanipulator (WR-6, Narishige, Japan). Patch pipettes were pulled from glass capillaries using a Narishige puller (Narishige Co. Ltd, Tokyo, Japan), fire polished, and had a resistance of 3–5 MΩ for whole-cell recordings and 5–7 MΩ for single-channel recordings. The pipettes were filled with 140mM KCl, 10mM HEPES, 1mM $MgCl_2$, 5mM EGTA, and 4.9M $CaCl_2$ buffered to pH 7.2 by adding KOH. Cells were super-perfused with a bath solution containing 140mM NaCl, 5mM KCl, 1.2mM $MgCl_2$, 10mM HEPES, 10mM glucose, and 2.4mM $CaCl_2$. Following gigaseal formation, bath solution was switched to the following: 140mM KCl, 10mM HEPES, 1mM $MgCl_2$, 5mM EGTA, and a desired free Ca^{2+} concentration which was adjusted by adding different amounts of $CaCl_2$ buffered to pH 7.2. (Bondarenko et al. 2011, Bondarenko et al. 2013). Single-channel activity was expressed as *N*Po, where *N* represents the number of functional ion channels in the membrane patch and Po represents the open channel probability determined from idealized traces (Bondarenko et al. 2011). *N*Po was obtained from ≥20s of continuous recording under each experimental condition. The effect of VSN16R was estimated after 3 min of continuous exposure to VSN16R-containing solution. Data was analysed by ANOVA was performed, and statistical significance was evaluated using Scheffés post-hoc test of the Prism 5 software for Windows (GraphPad Software).

Pharmacokinetics. The stability to hepatic and plasma degradation was assessed *in vitro* by Inpharmatica, Cambridge, UK. Compounds (1μM) were incubated with either pooled mouse liver microsomes (0.1mg protein/mL) or pooled mouse plasma at 37ºC for 0, 5, 10, 20 and 40 minutes before termination with acetonitrile containing warfarin as an analytical internal standard. Samples were centrifuged and the resultant supernatant analysed for parent compound. The mass responses at baseline were taken as the 100% reference values against which the disappearance of compound was measured. The natural log of the % remaining values was used to generate linear plots of disappearance of the compounds. Half-life values

were calculated from the slope of these plots. Hepatocyte metabolism was assessed by Cyprotex, Macclesfield and 10μM VSN16R was incubated with primary mouse, rat, monkey (Macaque) and human hepatocytes for 1h and the presence of metabolites was assessed using liquid crystallography mass spectroscopy. The stability of VSN16R was assessed *in vivo* by Inpharmatica, Cyprotex and Charles Rivers, Cambridge. Blood (plasma) samples were obtained prior to and 5min-24hours after drug administration of 2-5mg/kg i.v. or 5mg/kg p.o. VSN16R into outbred mice and rats (n=three per time-point). In addition plasma samples, brain and spinal were obtained from ABH with spastic EAE. Immediately after blood collection the brain and spinal cord were removed and then stored at -20°C prior to assay. Tissue samples were weighed, homogenized and centrifuged and the lysates generated. Brain lysates and plasma were assayed by LC-MS methods by Inpharmatica/Charles Rivers, Cambridge, UK. This was also performed using a Waters Xevo TQ or API4000, AB Sciex mass spectrometer using spiked samples as standards. PK Solutions Software (Summit Research Services, Montrose, CO, USA), AB Sciex Analyst software combined with Thermo Fisher Scientific Watson LIMS processing and reporting software or WinNonLin pharmacokinetic or PK solutions 2.0 software (Summit Research Services, Montrose CO, USA) were used to produce PK parameters. Data is expressed as mean ± SEM. The detection limit of VSN16R was 2ng/mL in plasma and brain and 14ng/mL in spinal cords. The detection limit of VSN22R was 2ng/mL in plasma and 0.1ng/mL for VSN44R in plasma. Pharmacokinetics in toxicological samples in rats (n=six/group), dogs (n=six/group) and humans (n=six/group) was performed by Charles Rivers, Edinburgh, UK.

Open-Field Activity Monitoring: Motor activity was assessed using a 27.9cm x 27.9cm open field activity monitor chambers and computer software (Med Associates Inc, St. Albans, VT, USA.). This was typically performed in a darkened room. Recording were initiated once the mouse entered the chamber and continued for 5 minutes. These chambers, allowing 4 simultaneous recordings of individual mice, were fitted with infrared beams that could detect movement in the X, Y planes. The total distance travelled (cm) was recorded. Results were expressed as mean ± SEM. These were analysed by a paired Students t test or a one way ANOVA with Bonferroni post hoc test, using SigmaStat V3/Sigmaplot V9 or V11 software (Systat Ltd Hounslow, UK.Al-Izki et al. 2012).

Temperature Testing. Temperature was monitored by using a thermocouple placed under the hindlimb and the temperature was allowed to equilibrate for and was recorded once the temperature failed to increase further (Pryce et al. 2014). These were assessed 20 minutes following administration of compounds. Results were expressed as mean ± SEM. These were analysed by students test a one way ANOVA with Bonferroni post-hoc test using Sigma/StatV3/Sigmpaplot V9 or V11 software (Pryce et al. 2014).

Induction of Spasticity. Disease was induced by immunization with spinal cord homogenate in Freunds adjuvant as described previously and included data relevant to the ARRIVE guidelines related to EAE induction (Al-Izki et al. 2012, Pryce et al. 2014). Following the development of chronic relapsing EAE, spasticity typically developed after 2-3 relapses, about 80-100 days post-induction onwards as a consequence of the accumulation of nerve damage (Baker et al. 2000, Al-Izki et al. 2012). This was assessed in non-anaesthetized, awake animals during remission from active paralytic episodes by the force required to bend the hind limb to full flexion against a custom built strain gauge, following extension of the limb prior to measurement. This cannot be used on limbs that are flexed, which were not measured. Animals with visible spasticity were used as spasticity became apparent. The data was analyzed using Spike 2 software (Cambridge Electronic Design, UK) and a mean score for each limb at each time point was calculated and forces were converted to Newtons (Baker et al. 2000, Pryce et al. 2014). Animals were entered into study following the development of visible spasticity. These mice were randomly assigned to treatment group by the person administering the compounds or vehicle and mice were assessed in a blinded fashion by a different assessor. Data was analysed blinded to treatment. Each group contained a minimum of five different animals. This would provide 80% power to detect a 25% change in limb (n=ten) stiffness at the $P<0.05$ level, as reported previously (Pryce et al. 2014). The results represent the mean ± SEM resistance to flexion force (N) or individual limbs, which were compared using one way repeated measures ANOVA incorporating a Student-Newman-Keuls post hoc test or infrequently paired t tests using SigmaStat V3/Sigmaplot V9 or V11 software (Pryce et al. 2014). Resistance forces of limbs below 0.15N were typically excluded from analysis, as this is below normal range on non-spastic limbs (Baker et al. 2000) consistent with a pre-defined protocol. Differences were compared to baseline using repeated measures analysis of variance rather than comparison of group means, because there is such marked heterogeneity in the severity of spasticity in individual limbs, resulting in variable baseline group means, as shown previously (Baker et al. 2000). Therefore, to assist in comparison, data was sometimes also expressed as percentage change ± SEM from baseline.

Electrophysiology. Animals with spasticity were anaesthetized using 50mg/kg ketamine (Modol et al. 2014) and 1mg/kg dexmedetomidine/medetomidine according to veterinary advice. The experiment was terminated, without recovery, prior to loss of anaesthesia. A drop of 2% hyroxypropyl methylcellulose was added to the eyes to prevent drying. The animal was secured in a stereotactic frame and body temperature was maintained at 37°C with a small heating plate with built in resistance temperature detector sensor connected to a direct current temperature controller linked to an anal thermocouple. The legs and nape of the neck were shaved and the sciatic nerve in the upper thigh was surgically exposed. The animal, at the nape of the neck, and heating pads were earthed using electrodes. The animal was covered to conserve

heat. The stimulating electrode was placed under the sciatic nerve and sealed with white petroleum jelly. Stimuli of 100 ms duration constant current were delivered to the sciatic nerve using a Neurolog NL800 (Digitimer), at a rate of 0.2 Hz, and the current increased until a convincing recording of both M-wave (stimulus from electrode to muscle) and H-wave (stimulus from the electrode to the spinal reflex arc and from motor nerves to muscle approximately 7ms after the M wave (Modol et al. 2014) were generated in each sweep. The current required varied from preparation to preparation, but was substantially less than that eliciting a supramaximal nerve activation (current range ≈ 1 mA. (Modol et al. 2014)) Differential motor unit recording from anterior tibialis was achieved using a Neurolog AC preamplifier and headstage (Digitimer, Welwyn Garden City, UK). Two monopolar 25 gauge needle recording electrodes were inserted into the muscle at either end, the signal was amplified, band-pass filtered between 200 Hz and 1 KHz, digitized by a 1401 plus interface (at 3 KHz) and then displayed, and saved by a computer running Signal software (Cambridge Electronic Design). 30mg/kg VSN16R or 0.1mL PBS was injected i.v. via the tail vein. This route was selected as it could be administered without further movement of the animal and disturbance of the recording electrodes. The high starting dose was selected based on the amount of VSN16R that could easily be dissolved in saline to maximize duration, as a starting point. The response for 12 minutes was recorded, although once detected the H response was maintained without attenuation for over a 30minute observation period. The amplitude (mV) was measured and compared to 100% at time of injection, rather than a mean response due to variability in the current required to the maximal H response.

RNA extraction and sequencing. Three EAE mice demonstrating spasticity and three age-matched control mice were killed and spinal cord tissue was removed, snap-frozen and stored at -80ºC. These were analysed by RNAseq as described previously (Sevastou et al. 2016). Frozen tissue was disrupted in TRIzol® Reagent on ice, using a rotor-stator homogeniser. Following 5 min incubation at room temperature, chloroform was added to the samples, which were shaken, left to rest and then centrifuged at 12,000 g for 15 minutes. The resulting upper aqueous phase was washed with 70% ethanol, mixed well and loaded on an RNeasy column. Thereafter the Qiagen RNeasy® Mini Kit protocol was followed to extract and purify mRNA. The mRNA integrity was assessed by microfluidic capillary electrophoresis using the Agilent 2100 Bioanalyzer. All samples had a 260/280 ratio > 1.8 with RNA integrity number > 9. RNA sequencing was performed at the UCL Genomics facility (UCL Institute of Child Health, London) using the Illumina NextSeq 500 platform. The FASTQ files generated for each sample were aligned to the UCSC *Mus musculus* HG19 reference genome using the TopHat2 software (Illumina). Downstream analysis of these alignments was performed using Cufflinks software (Illumina). Cufflinks computes normalized fragments per kilobase of exon per million fragments mapped (FPKM), which reflect the expression levels of each mRNA molecule. The reads were mapped to a total of 23,352 genes and 30,608 transcripts. The statistical

analysis resulted in p values corrected for multiple testing with a default false discovery rate of q<0.05 (Sevastou et al. 2016).

Western Blotting. Mouse spinal cord whole tissue was homogenised in RIPA buffer (150 mM NaCl, 1.0% IGEPAL CA-630, 0.5% sodium deoxycholate, 0.1% SDS, and 50 mM Tris at pH 8.0), supplemented with protease and phosphatase inhibitors (Sigma, Poole Dorset). Similarly, EA.hy926 cells were lysed in RIPA buffer supplemented with protease and phosphatase inhibitors. The proteins were resolved on sodium dodecyl sulfate–polyacrylamide gel electrophoresis gels and transferred onto Immobilon-P-polyvinylidene difluoride membranes. Membranes were washed, blocked for 1 h in blocking buffer (5% non-fat dried milk) and incubated in blocking buffer with primary antibody using rabbit polyclonal antibodies against mouse/human KCNMA1 (APC-021, previously validated by lack of activity in big conductance calcium activated potassium channel *Kcnma1*-deficient mice, and APC-151 antibody) and KCNMB4 (APC-061 Antibody, previously validated by lack of activity in *Kcnmb4*-deficient mice despite detecting multiple isoforms), which were purchased from Alomone Labs, Jerusalem Israel, whose website reports supporting literature concerning characterization of the antibodies. These were incubated overnight at 4^{o}C at 1:200 dilution or mouse monoclonal antibodies incubated for 2h at room temperature (anti-β-actin. 1:2000, Santa Cruz BioTech sc-101663). After repeated washes in Tris buffered saline with Tween 20 (T-TBS; 10 mm Tris-HCl, 150 mm NaCl, and 0.5% Tween 20, pH 7.4), membranes were incubated with Horse radish peroxidase-conjugated secondary antibody (anti-rabbit Immunoglobulins 1:4000, Santa Cruz BioTech sc-2004 or anti-mouse Immunoglobulins 1:1000, ThermoFisher. SA1-100) in T-TBS for 1h. Blots were developed by enhanced chemiluminescence detection.

Data and Statistical Analysis. The data and statistical analysis comply with the recommendations on experimental design and analysis in pharmacology (Curtis et al. 2015). Most experiments contained a minimum of ≥ 5 animals or individual samples, consistent with sample size calculations and experience from previous studies, as indicated. Group sizes of less than n = 5 were used in some pharmacokinetic studies, based on a minimum numbers approach. However, rodent pharmacokinetic studies were replicated in additional experiments. The statistical tests used, are reported in the methodological subsections. If this involved parametric analysis, this included analysis of normality and equality of variance. The level of probability deemed to constitute the threshold for statistical significance was $P<0.05$.

Nomenclature of Targets and Ligands. Key protein targets and ligands in this article are hyperlinked to corresponding entries in http://www.guidetopharmacology.org, the common portal for data from the

IUPHAR/BPS Guide to PHARMACOLOGY (Southan et al., 2016), and are permanently archived in the Concise Guide to PHARMACOLOGY 2015/16 (Alexander et al., 2015a, 2015b, 2015c).

RESULTS

VSN16 is a novel anti-spastic agent.

Following the synthesis of VSN16, the CB_1R affinity of VSN16 (racemate) was first assessed by measuring the relaxation of electrically-evoked contraction of the vas deferens (Ross et al. 2001) This is a standard, tissue-based assay used to detect cannabinoid receptor activity (Ross et al. 2001), but assesses autonomic neurotransmission for a wide range of receptors, via actions on nerves originating from pelvic and lumbar/sacral ganglia (Burnstock & Verkhratsky 2010). VSN16 exhibited potent inhibitory activity with an EC_{50} in the low nM (~10nM) range (Figure 1A). This compared favorably with the potent CB_1R/CB_2R agonist *R*(+)WIN55-212 (Figure 1B), although the slope of the VSN16 dose-response curve (Figure 1A) appeared different, possibly suggesting activity at a distinct target or targets. VSN16R did not affect beta gamma, methylene adenosine triphosphatase-induced contraction in electrically unstimulated vasa deferentia (Supplementary Data. Figure S2), indicating the action of VSN16R was not directly on the muscle. Although VSN16 was at least as potent as *R*(+)WIN55-212 (Figure 1A, B), it failed to induce visible signs of sedation at 1mg/kg i.v. and did not induce hypomotility (Figure 1C) or hypothermia (Figure 1D, which are indicative of central cannabimimetic effects in rodents (Varvel et al. 2005). This contrasts to the sedative effects ($P<0.001$) induced by *R(+)*WIN55-212 (Figure 1C, 1D), which are absent in CB_1R-deficit mice (Pryce et al. 2014). Whilst, the action of VSN16 could be antagonized following pretreatment of the vas deferens with SR141716A, a CB_1R antagonist (Figure 1A), when VSN16R was injected directly into the CNS, it also failed to induce cannabimimetic effects (Figure 1D), clearly indicating that VSN16 was neither a global, nor a CNS-excluded CB_1R agonist *in vivo*, at the doses tested and thus was active by another SR141716A-sensitive mechanism.

In MS, spasticity is measured via subjective assessments that are either physician-assessed, such as the modified Ashworth Scale or patient-assessed numerical rating scales (Shakespeare et al. 2003, Novotna et al. 2011, Winiger et al. 2015). These are limited compared to objective measures and may be poorly responsive to treatments (Shakespeare et al. 2003, Novotna et al. 2011, Winiger et al. 2015). Although spasticity in mice was visually evident, it was objectively and quantitatively measured using a strain gauge to detect limb stiffness (Baker et al. 2000). Interestingly it was found that 1mg/kg i.v. VSN16 could significantly ($P<0.001$) inhibit spasticity within a few minutes of administration (Figure 1E) and occurred in the absence of sedative effects (Figure 1C, D). As VSN16 is chiral, both the R and S enantiomers were made and VSN16R (EC_{50}= 10nM) was slightly more active than VSN16S (EC_{50}=37nM) in the mouse vas deferens assay, as was also subsequently seen in the vasorelaxation of rat mesenteric arteries, which is another standard tissue-based assay used to measure vascular cannabinoid receptor activity (VSN16R EC_{50}=110nM, VSN16S = 140nM (Hoi et al. 2007)). However, when the *in vivo* pharmacokinetic responses

were assessed in both outbred mice and rats (Figure 1F), clearance of VSN16R administered via the i.v. was relatively fast (Half-life of 7-11min respectively). This demonstrated CNS penetration with a plasma:brain ratio at C_{max} of 0.16 in healthy mice (Figure 1E). It was found that VSN16R appeared slightly more active than VSN16S in spasticity when tested at 5mg/kg i.v. (Figure 1G) and therefore subsequent studies focused on VSN16R. 5mg/kg i.v. VSN16R could induce comparable inhibition of spasticity to 5mg/kg i.v. baclofen (Figure 1H), although this dose of baclofen was associated with significant sedation (Figure 1C, D). Likewise, VSN16R appeared to be as potent as 5-10mg/kg i.v. (sedative) doses of the botanical drug substances in nabiximols/medicinal cannabis (Figure 1H. Hillard et al. 2012). Therefore, whilst VSN16R may be no more potent than current anti-spastic agents, it lacked their sedative capacities, which limits compliance and early use in spasticity in MS.

VSN16R is an orally-active, anti-spastic agent.

In contrast to the i.v. route, the delivery of 5mg/kg via the oral route showed a longer elimination half-life in rodents (89min in mice and 43min in rats (Figure 1E)). Oral absorption was rapid and C_{max} was detected within 15min from administration in mice indicating good absorption from the gastrointestinal tract and good oral bioavailability (22-40% mouse-rat, respectively, after 5mg/kg p.o.) was evident (Figure1F). Doses of up to 30mg/kg i.v. VSN16R in PBS failed to show any visible evidence of sedation in mice (n=five animals) and repeated daily treatment of 1g/kg p.o. in water mice for 5 days failed to show any overt behavioural effects or toxicity and no drug-induced weight loss (29.0 ± 2.0g vs. 30.2 ± 1.1. n=three mice). Oral VSN16R was very-well tolerated in rats also and behavioural testing of rats treated with 120mg/kg p.o. (n=six) did not display any adverse behavioural responses in Irwin tests (Roux et al. 2005), which assesses over 30 largely, neurological and movement, behavioural outcomes (Supplementary data. Table S1).

The action of oral VSN16R was analyzed in spasticity in ABH mice with EAE (Figure 2). Whilst 0.5mg/kg p.o. VSN16R failed to produce rapid muscular relaxation and inhibition of spasticity (Figure 2A), significant therapeutic activity was evident within 10min following administration of 1mg/kg VSN16R p.o. (Figure 2A) and 5mg/kg VSN16R p.o. (Figure 2A). Therefore, VSN16R has over a one thousand fold therapeutic window. Despite the marked variability in spasticity in individual limbs (Figure 2B), which could influence group means depending on which animals were assessed (Figure 2C, 2D), it was evident that most limbs showed significant level of relaxation irrespective of the degree of initial spasticity when treated with 5mg/kg p.o. VSN16R (n=17 animals, 32 = limbs. Figure 2B). The duration of activity was dose-dependent and inhibition of spasticity lasted for over 6h following a single dose of 40mg/kg p.o. (Figure 2C). Furthermore, the therapeutic effect was sustained after repeated daily 40mg/kg p.o. VSN16R

administration for 7 days (Figure 2D). This suggested the lack of significant receptor desensitization and even suggested some cumulative benefit as following repeated administration there was significantly reduced spasticity compared to starting values 7 days earlier (Figure 2D. n= fifteen limbs from eight mice). However, spasticity returned to baseline levels following cessation of treatment (Resistance to Flexion Force Baseline 0.174 ± 0.033N. 2 weeks after cessation of weekly VSN16R treatment 0.157 ± 0.045N mean± SEM (n=ten limbs from six animals. Two animals reached humane endpoints after termination of VSN16R dosing). Repeated daily vehicle failed to influence the degree of spasticity (Figure 2E). However, in contrast to lack of desensitization with repeated VSN16R (Figure 2D), repeated 5mg/kg p.o. baclofen ($GABA_B$ agonist, Figure 2E) and 25mg/kg subcutaneous CNQX (AMPA/Kainate glutamate receptor antagonist, Figure 2F) showed inhibitory responses that diminished over time (Figure 2E, 2F). This was indicative of receptor desensitization and supports the need to dose-escalate baclofen when used in humans (Shakespeare et al. 2003). Furthermore, in contrast to loss of muscle tone in healthy animals that can occur following sedation (Supplementary data. Figure S3), 40mg/kg p.o. caused no loss of muscle tone in normal animals (9.1% ± 6.3% change (increase) from baseline n=six animals (P=0.274) compared to 17.8% ± 5.3% drop n=eight animals. P<0.001 compared to baseline using repeated measures ANOVA, in visibly spastic animals). In this analysis (Figure 2A-2F) each limb was treated as the unit of assessment, to encompass the marked variability of spasticity in different limbs (Figure 2B) and offers 3Rs value to limit animal use (Baker et al. 2000). However, to address concern of pseudo-replication via analysis of both limbs, when only one mean result per animal was assessed, again 0.1mL vehicle failed to influence spasticity (p= 0.217. n= 17 animals) and again 5mg/kg p.o. significantly (P<0.001 at 30min, 60min) inhibited spasticity (n= 17 animals) when compared to baseline (Figure 2G). Furthermore, whilst the mean group score (± SD) in vehicle-treated animals (0.278 ± 0.078N) was no different to the baseline of animals treated with 5mg/kg p.o. (0.302 ± 0.073N), animals were significantly less spastic 30min (0.224 ± 0.067N). and 60min (0.214± 0.071N) following treatment with 5mg/kg p.o. compared to vehicle-treated animals (Figure 2G).

The Hoffman (H) reflex, where the spinal reflex is highly exaggerated due to over excitation/loss of descending inhibitory tone following the CNS damage that causes spasticity (Matthews 1966, Baker et al. 2012) was assessed (Figure S3). Whilst it is often used in experimental spasticity studies (Modol et al. 2014), electrophysiology may not always detect anti-spastic effects in humans and does not always yield consistent results (Leocani et al. 2015). Whilst the H reflex following stimulation of the sciatic nerve and recording from the anterior tibialis muscle (Modol et al. 2014) could be variably detected and modified by VSN16R in some animals, this was not consistent (Figure 3S). Furthermore, this approach was considered of limited value as it was clear that the ketamine (NMDA antagonist) and medetomidine/dexmedetomidine

hydrochloride (alpha 2 adrenergic receptor agonist) anaesthetics typically used (Modol et al. 2014), inhibited physical spasticity and importantly the anaesthetics were found to block the mechanism of action of VSN16R (Figure 3S). Furthermore, the animals, which are severely neurologically affected could not tolerate the anaesthetic procedure, unlike healthy mice, often causing death. Therefore the approach was terminated on ethical grounds.

It was clear from pharmacokinetic studies in mice that there was over 15% CNS penetration with VSN16R, even at low doses (Figure 1F). Given the high doses of VSN16R that could be administered it was evident that brain penetration of VSN16R was not inducing abnormal behavioural effects (Supplementary data. Table S1), consistent with the direct CNS injection of VSN16R (Figure 1D). Furthermore, CNS penetration is increased during spastic EAE, due to blood brain barrier dysfunction (Al-Izki et al. 2014). As such a CNS-excluded CB_1R-agonist (10mg/kg i.v. CT3 (Pryce et al. 2014)) induced significant ($P<0.001$) cannabimimetic effects in spastic animals (2.3 ± 0.4˚C temperature loss, 20 minutes after administration. n=six mice) at doses that did not affect healthy mice (0.0 ± 0.1˚C. n= five mice). In addition it was possible to detect VSN16R in spinal cords of chronic EAE animals (Brains four/four mice. Spinals cords n=two/four mice) compared to normal animals (Brains n=four/four mice, Spinal cord n=zero/four mice), despite lack of sensitivity of the assay, indicating that there is some additional lesional targeting of VSN16R during EAE, as has been seen previously with other compounds that are not fully CNS-penetrant (Al-Izki et al. 2014). The duration of action showed a reasonably good correlation with the pharmacodynamics of plasma levels of VSN16R in ABH mice with EAE (Figure 2H). Similar plasma levels of drug could easily be achieved and exceeded with comparable doses of VSN16R in healthy humans (Figure 2F).

Metabolism of VSN16R produces biologically-active metabolites.

Pharmacokinetic studies have indicated rapid absorption of VSN16R in rodents (Figure 1F). Renal excretion accounted for less than 0.5% of the administered dose and faecal elimination was approximately 1% of the dose in the first 12h following oral dosing of rats (n=three). VSN16R was stable (t½ >100min which was the upper limit for assessment) in liver microsomes and plasma, compared to midazolam (t½ = 17 min) in liver microsomes and Bisacodyl (t½ = 2 min) in plasma. VSN16R showed no significant inhibition of cytochrome p450 enzymes at 10µM suggesting limited potential for drug-drug interactions (Supplementary Data. Table S2). However, when VSN16R was incubated with mouse, rat, dog, monkey and human hepatocytes, and the supernatants assessed by LC-MS 1h later, two dominant metabolites from mouse hepatocytes were identified and synthesized (Figure 3A). (R,Z)-N-(1-hydroxypropan-2-yl)-3-(6-(methylamino)-6-oxohex-1-en-1-yl)benzamide (Molecular weight = 304 Da), named VSN22R, resulted

from demethylation of the N-dimethyl amino group of VSN16R. Oxidation of the terminal alcohol group to form a carboxylic acid produced (Z)-(3-(6-(dimethylamino)-6-oxohex-1-en-1-yl)benzoyl)-D-alanine (Molecular weight = 332 Da), which was named VSN44R (Figure 3A). VSN22R and VSN44R were tested in the electrically-evoked contraction assays of the mouse vas deferens and it was found that VSN22R had comparable affinity (EC_{50} = 9nM) to VSN16R (EC_{50} = 10nM), whereas VSN44R was significantly more potent (EC_{50} = 1nM) (Figure 3B). In contrast, they all had comparable activity (EC_{50} = ~100nM in relaxing methoxamine-evoked contraction of third order mesenteric artery contraction (Figure 3C). However, given the activity in the tissue-based assays (Figure 3B, C), it was not surprising that both VSN22R and VSN44R could inhibit the spasticity during EAE (Figure 3D). This indicates that they should contribute to the pharmacological effect of VSN16R *in vivo*.

VSN16R is well-tolerated at drug levels achievable in humans.

Studies indicated that mice tolerate 1000mg/kg p.o. and likewise, independent, toxicology studies indicated that the No Evidence of Adverse Events Level (NOEL) was 1000mg/kg p.o. in rats over 28 days (n=twenty). The NOEL was 150mg/kg p.o. in rabbits and 100mg/kg p.o. in dogs (n=six) with reproductive toxicology safe levels at 1000mg/kg p.o. in rats (n=nine) and >500mg/kg in rabbits (n=nine) and there was no evidence of mutagenesis in a standard Ames test (Supplementary Data. Table S3). In rats there was occasional evidence of salivation and "ploughing" behaviours, and there was evidence of salivation and vomiting in dogs at doses of 200mg/kg p.o. Likewise, rabbits demonstrated evidence of loss of appetite and loss of weight at higher (>150mg/kg) doses of VSN16R. These behaviours can be associated with poor taste. This aspect was avoided by encapsulation of drug for human use and no vomiting or issues of taste were reported in human studies (n=sixty). Histological analysis of animal (>30) tissues showed essentially no significant microscopic findings attributable to VSN16R (Supplementary Data. Table S4) and there were not cardiovascular issues (Supplementary data. Table S5). The drug was therefore very well tolerated in animals. Analysis of plasma levels of a therapeutic 5mg/kg p.o. dose of VSN16R in ABH mice with spastic EAE, indicated that there was only 73.0 ± 6.1 ng/mL of VSN16R, 106 ± 6.1 ng ng/mL VSN22R and only 2.1 ± 0.3 ng/mL VSN44R present (n=4). This plasma level of VSN16R and its metabolites was easily achievable in rats (Figure 4A) and dogs (Figure 4B) in toxicological studies and safety studies in humans (Figure 4C, D). Thirty minutes following 50mg/kg p.o. the amount of VSN16R detected in plasma (Mean ± SD) was 4,907 ± 32.3 ng/mL (15µM) in rats (n=six) compared to 26,150 ± 1,557 ng/mL (82µM) in dogs (n=6). At C_{max} typically at 30min following 1000mg/kg p.o. there was up to 117,000 ± 5,710 ng//mL (368µM) VSN16R in rats (n=eight) and at 200mg/kg p.o. there was 105,283 ± 13,309 ng/mL VSN16R in dogs (n=six) and therefore animals could tolerate high levels of VSN16R.

VSN16R is well-tolerated in humans.

Healthy male volunteers 18-50 years old (Supplementary data. Table S6) were randomly allocated to treatment in double-blind, placebo-controlled, phase I studies (EudraCT 2013-002765-18). This consisted of a single ascending dose (SAD) study of 25mg, 50mg, 100mg, 200mg, 400mg and 800mg in groups of eight different people per dose with six people given active drug in either 25mg or 100mg gelatine capsules (Figure 4C). No serious adverse drug-related events occurred and treatment was largely unremarkable in all cases. Any adverse events reported (14.3% in SAD) were mild and none were considered to be definitively-related to VSN16R, although no adverse event was recorded in people treated with placebo capsules. However, 5/42 VSN16R-treated subjects (11.9%) were considered to have a possible relationship to treatment and these included dizziness (1 subject at 25 mg & 50mg), headache (1 subject at 200 mg) and dyspepsia and nausea (at 800 mg). Haematology and serum biochemistry (Supplementary data. Table S7), coagulation, urinanalysis, vital signs and electrocardiograms (Supplementary data. Table S8) and blood pressure (10min in a supine position or after 1 min standing. Supplementary Data. Table S9) remained unremarkable. Plasma was repeatedly sampled and pharmacokinetic studies demonstrated the rapid presence of VSN16R indicating good gut absorption, with 100% bioavailability at 25mg and a terminal elimination of 3.4-4.9h over the dose range studied (Figure 4C). Even at the lowest 25mg drug dose tested, it was clear that plasma levels were well above plasma levels of therapeutic 5mg/kg p.o. doses in mice and these were achieved for a number of hours (Figure 4C, 4D). Formation of metabolites was rapid and it was found that VSN22R was the dominant metabolite species in humans and once generated levels were similar to those found with VSN16R and had a terminal elimination half-life of 4.0-5.3h across the dose range tested (Figure 4A-C). Again VSN44R appeared at ten to a hundred fold lower levels (Figure 4A-C). These data suggest that even in the absence of a slow-release formulation, twice (b.i.d)-thrice daily drug delivery could probably achieve steady state of therapeutic drug levels (Figure 4F). In addition the trial contained a multiple ascending drug dose study of twice daily 25mg, 100mg and 400mg in groups of eight different fasted people per dose with six people given active drug in either 25mg or 100mg gelatine capsules was performed (Figure 4D). Again, the drug was well tolerated and the pharmacokinetics resembled that following the SAD studies (Figure 4C, D, E). It was found that six/eighteen VSN16R-treated subjects (33.3%) and to two/six (33.3%) placebo subjects reported adverse events and three/eighteen VSN16R-treated subjects (16.7%) were considered to have a possible relationship to treatment, although again none was considered to be definitely related to drug treatment. These people reported oropharngeal pain and rhinitis (at 25 mg b.i.d), abdominal distension (at 25 mg b.i.d) and abdominal pain and nausea (at 400 mg b.i.d). There were no serious adverse events. Following twice daily dosing steady state plasma levels above 100nM for both VSN16R and VSN22R, likely to be therapeutic, could be achieved in healthy individuals (Figure 4D). Initial studies were in fasted individuals (Figure 4C, 4D, 4E) and therefore studies were

undertaken following feeding with 0.5h of dosing. Whilst this delayed T_{max} and reduced C_{max} the extent of absorption (total exposures) was not influenced and if anything, feeding improved the therapeutic levels of VSN16R and its metabolites (Figure 4F). This data indicates that VSN16R is well tolerated in humans and does not induce sedation.

VSN16R targets BK_{Ca} potassium channels independently of G-protein coupled cannabinoid receptors. Whilst VSN16R was a safe and potent anti-spastic agent, the mechanism of action was not initially obvious, as early in the studies it was recognised that, despite being antagonised by SR141716A/rimonabant (Figure 1A), VSN16R does not bind to or agonize CB_1R in receptor-transfected cell line-based assays (Supplementary data Figure S5). Furthermore, VSN16 could still inhibit spasticity ($P<0.001$) in global CB_1R-deficient ABH mice (Figure 5A). Therefore, the action of VSN16R was clearly independent of CB_1R. In addition, VSN16R did not bind (tested to 10 µM) to CB_2R or other parts of the endocannabinoid and endovanilloid system (tested to 10 µM) and a wide range of receptors and transporters (Supplementary Data. Figure S5).

Although SR141716A and AM251 are CB_1 cannabinoid receptor antagonists, they have additional off-target effects associated with a non CB_1/CB_2 vascular target for anandamide (Ho & Randall 2007, Pertwee et al. 2010). They and O-1918 could antagonize the action of VSN16R in mesenteric artery relaxation assays (Hoi et al. 2007), which were used to help identify the target for VSN16R activity. It has been reported that O-1918 can target GPR18 and GPR55, as candidates for a putative non-CB_1R/CB_2R vascular cannabinoid receptor that is activated by some endocannabinoids (Baker et al. 2006, McHugh et al. 2010; Bondarenko 2014). Stimulation of this vascular target has been associated with the development of low blood pressure in some studies (Bondarenko 2014), however it was clear that VSN16R did not induce hypotension in rodents (Hoi et al. 2007), dogs and humans (Supplementary data Table 5S, Table S9). GPR18 and notably GPR55 are bound by SR141716A and AM251 (Baker et al. 2006, Pertwee et al. 2010). However, as the action of VSN16R is *Bordetella pertussis* toxin insensitive, the vasorelaxing effect of VSN16R is not mediated by GPR18 (Hoi et al. 2007). Furthermore, VSN16R does not directly bind to GPR55 either (tested in Multispan C1113, Multispan H113, HEK293T.*GPR55* cells lines and mouse DBT.*Gpr55* cell lines in a variety of different assays including calcium signalling, receptor internalization and nuclear localization of cAMP response element binding protein (Supplementary data. Figure S5)). Importantly VSN16R continued to inhibit spasticity in GPR55-deficient ABH mice (Figure 5B). Therefore, other O-1918 reactive targets were examined.

Although VSN16 was originally designed as an anandamide analogue, it is also structurally similar to N-arachidonoyl glycine and N-arachidonoyl serine (Supplementary data. Figure S1). Arachidonoyl glycine is an endogenous ligand of GPR18 that causes vasorelaxation, which is blocked by 0-1918, via stimulation of a presumed G-protein coupled vascular receptor (Parmar & Ho. 2010). However, this appears to directly activate big conductance calcium-activated potassium (BK_{Ca}) channels (Bondarenko et al. 2013). Likewise N-arachidonoyl serine that may act on GPR55 can inhibit vasorelaxation by endothelial cell-dependent and independent mechanisms following direct BK_{Ca} activity that was directly blocked by 0-1918 (Godlewski et al. 2009). This suggested that BK_{Ca} may mediate the vasorelaxing effects of at least some cannabinoids (Bondarenko 2014). VSN16R did not affect primary porcine aorta endothelium (Supplementary data. Figure S4), but in assays in third order rat mesenteric arteries, VSN16R could induce significant vasorelaxation in an endothelium-dependent manner (Figure 5C) and was significantly inhibited by antagonists of BK_{Ca} channels, notably by Iberotoxin and charybdotoxin. Apamin (Small conductance $SK_{Ca}2/3$ KCNN2/KCNN3 channel antagonist) alone had a small inhibitory effect on VSN16R function in the mesenteric artery assay (Figure 5D), but VSN16R failed to block binding of apamin to $SK_{Ca}2$ KCNN2 channel in transfected cells (Supplementary data. Figure S5). In addition, the relaxation was dependent on potassium flux, as VSN16R produced no relaxation in the presence of extracellular 60mM KCl, supporting an action via BK_{Ca} channels (Figure 5C).

This target was definitively shown in single channel, inside-out patch clamp experiments in human EA.hy926 cells (Bondarenko et al. 2011), where VSN16R (n=seventeen patches), VSN22R (n=twenty-two patches) and VSN44R (n=four patches) all facilitated single BK_{Ca} channel activity when applied to the inner surface of the membrane (Figure 5E). The increase in *N*Po occurred in a concentration, calcium-dependent and voltage-dependent manner (Figures 5F, G. Supplementary data Figure S3), indicating that the compounds directly act as BK_{Ca} channel openers, without binding to other receptors. This caused hyperpolarisation of the membrane and importantly, this mechanism was active in human HCN-2 neural cells where VSN16R stimulated single BK_{Ca} channel activity in inside-out patches (Figure 5H), providing further evidence that VSN16R acts directly via neuronal BK_{Ca} channels (Figure 5H). Consistent with this, RNA*seq* indicated that EA.hy926 cells essentially only express the neural; KCNMA1, KCNMB4 BK_{Ca} isoform (Figure 6A). They did not express any of the leucine rich repeats containing (LRRC) BK_{Ca} gamma subunit proteins (Zhang & Yan 2014) or the STREX (Xie & McCobb 1998) steroid-responsive KCNMA1 splice variant (Figure 6A).

BK_{Ca} potassium channels are dysregulated during EAE and are a novel mechanism to control spasticity.

In the spinal cord the dominant BK_{Ca} subunits are the KCNMA1 alpha pore and the KCNMB4 beta chain, and KCNMB2 to a lesser extent and the LCCR52 gamma chain (Figure 6B). Surprisingly *RNAseq* analysis of spinal cords from spastic and age-matched controls (n=three) failed to detect significant differences in the expression of any of the BK_{Ca} subunits (Figure 6B), consistent with KCNMA1-specific western blot of spinal cords (Figure 6B). Likewise, western blot of KCNMB4 in spinal cords did not indicate differences of KCNMB4 levels in spastic EAE, although additional bands, not present in EAE.hy926, became prominent in spastic mice with EAE (n=six) compared to controls (n=three), possibly due to disease-related post-translational modifications (Figure 6A), such as glycosylation (Jin et al. 2002). However, as spastic EAE is associated with significant nerve loss (Pryce et al. 2003), when KCNMA1 expression was normalized to neurofilament content there was a significant increase in the KCNMA1 (*Kcnma1*) to neurofilament light (*Nefl*) ratio in spastic mice (Figure 6B), suggesting some dysregulation during disease. However, blockade of the receptor, with paxilline did not influence the baseline level of spasticity (Figure 6C, 6D). Animals with deficiency in BK_{Ca} channels can exhibit adverse motor phenotypes and abnormal development that prelude their use in spasticity studies (Sausbier et al. 2004, Brenner et al. 2000, Martinez-Espinosa et al. 2014), therefore a pharmacological approach was used to investigate the action of BK_{Ca} in VSN16R biology (Figure 6C). It was found that 1mg/kg i.p. of the BK_{Ca} antagonist paxilline, which is just below a tremorogenic dose in mice (Imlach et al. 2008), could completely inhibit the action of VSN16R (Figure 6C). Furthermore, when structurally-unrelated BK_{Ca} openers were investigated in spasticity in EAE, it was found that BMS-204352, NS-1619 and NS-11021, used at published *in vivo* intraperitoneal doses, could all significantly inhibit spasticity (Figure 6D), without sedation and confirms that BK_{Ca} potassium channel openers provide a novel mechanism to control spasticity.

DISCUSSION

This study demonstrates that neural BK_{Ca} channels are a previously unrecognised target for control of spasticity in MS and other conditions. As such, compounds that support the opening of the BK_{Ca} channels and hyperpolarize neural membranes will limit neural excitability to control spasticity, in the absence of sedating side-effects. These could also potentially affect and may be of value in control of other MS symptoms or other conditions associated with neural hyperactivity and BK_{Ca} mutations: such as epilepsy, neuropathic pain, tinnitus and fragile X syndrome (Sausbier et al. 2004, Brenner et al. 2005, N'Gouemo 2014, Liu et al. 2015). Opening of the calcium-activated potassium channels form part of the neuronal repolarizing mechanism that helps re-set the ionic balance of the nerve to facilitate the generation of further action potentials (Sausbier et al. 2004, Brenner et al. 2005, N'Gouemo 2014). The observed upregulation of these channels in spinal cords probably contribute to facilitating the over-excitation of motor nerves leading to spasticity. As NS-1619, which is a KCNMA1-selective agent (Gessner et al. 2012), controls spasticity, this indicates that potassium-induced neural membrane hyperpolarisation following opening of the alpha pore in BK_{Ca} channels is the important mechanism of action. VSN16R also induces this mechanism and this will limit the generation of action potentials, to control spasticity.

Although VSN16R and NS-1619 both maintain the opening of BK_{Ca} channels, via the KCNMA1 pore, to produce membrane currents and are both blocked by the actions of Iberotoxin and SR141617A (White &, Hiley 1998), they have subtly distinct pharmacology and molecular targets (Hoi et al. 2007, White & Hiley 1998, Begg et al. 2003, Gessner et al. 2012). As such NS-1619 opens BK_{Ca} via a direct effect on the KCNMA1 pore of the channel and does not require the presence of KCNMB beta chains for activity (White & Hiley 1998, Gessner et al. 2012). Furthermore, in contrast to VSN16R, the action of NS-1619 can be resistant to the antagonistic effect of O-1918 (Gessner et al. 2012). As such NS-1619 relaxes mesenteric arteries via an additional, endothelial-independent mechanism that is due to an action on the KCNMA1 pore in smooth muscle that express the KCNMA1, KCNMB1 BK_{Ca} isoform (White & Hiley 1998, Brenner et al. 2000, Papassotiriou et al. 2000, Sausbier et al. 2004). VSN16R does not activate KCNMA1 directly or act via the smooth muscle BK_{Ca} isoform as shown here by: the endothelial cell dependence in induced arterial relaxation; the lack of relaxing effect of VSN16R on porcine aorta that express low levels of KCNMA1 and no BK_{Ca} beta chains (Papassotiriou et al. 2000) and the lack of effect on βγ-methylene ATP activity on smooth muscle. This is consistent with the lack of influence of VSN16R on blood pressure as seen in rats, dogs and humans, which is controlled by KCNMA1 and KCNMB1 on smooth muscle (Brenner et al. 2000, Sausbier et al. 2004, Zheng et al. 2013). Likewise VSN16R does not need the presence of BK_{Ca} gamma chains for activity. Therefore, although VSN16R activity is associated with membrane hyperpolarization that results from KCNMA1 pore opening, maintaining the opening of the

pore must occur via interactions of other elements (KCNMB4) of the BK_{Ca} channels. Skeletal muscles express only trace levels of BK_{Ca} (KNCMA1) and do not appear to express KCNMB1-4 (Freeman et al. 1998, Bednarczyk et al. 2013) and are therefore unlikely to be responsive to VSN16R. A neuronal action however, was indicated via the electrophysiological control of spasticity and the finding that a VSN16R-responsive cell line essentially only expresses a single KCNMA/KCNMB4 BK_{Ca} channel, which is the major neuronal BKCa isotype (Bednarczyk et al. 2013). The neuronal BK_{Ca} are found at high levels within sensory nerves, notably within dorsal root ganglia and spinal nerves (Freeman et al. 1998, Allen Brain Altas). There it may affect motor nerves or inhibitory interneurons, with or without influences on sensory outputs, as has been found with cannabinoid receptor agonists (Pryce et al. 2014).

Further work, will be required to determine the precise location and molecular function of VSN16R on BK_{Ca} channels during spasticity. This is however complicated as BK_{Ca} gene knockout animals exhibit adverse neurological phenotypes including: premature death; ataxia; tremors and gait and movement problems, which preclude their use in spasticity *in vivo* (Brenner et al. 2000, Sausbier et al. 2004). However, this may highlight new indications for treatment with VSN16R or related molecules. Furthermore the structural and electrophysiological biology of BK_{Ca} channels is highly complex because of their multimeric structure of alternatively-spliced and post-translationally modified alpha, beta, and gamma chains, which modulate both the expression of the alpha chain and the calcium and voltage thresholds of the alpha pore in both positive and negative ways (Brenner et al. 2000, Weiger et al. 2000, Sausbier et al. 2004, Zhang & Yan 2014). As such both gain and loss of function of the BK_{Ca} channels can lead to neural hyperexcitability (N'Gouemo 2014). The BK_{Ca} channels also appear to be part of the signalling machinery of some cannabinoid-related G-protein coupled receptors, such as GPR55 (Bondarenko et al. 2011, Bondarenko 2014) and potentially the CB_1 receptor (Sánchez-Pastor et al. 2014). In addition, being calcium-dependent, BK_{Ca} channel activity and VSN16R function may also be modulated secondary to alterations to intracellular calcium stimulation, or other intracellular signalling molecules, following activity of other receptors. This may be a mechanism by which SR141617A can inhibit BK_{Ca} activity in tissue assays (White & Hiley 1998). This type of activity may contribute to the confusion around the endocannabinoid pharmacology (Howlett et al. 2002, Pertwee et al. 2010, Bondarenko 2014). Additional actions of VSN16R cannot be excluded, especially since anandamide has a number of targets (Pertwee et al. 2010), but a large number of relevant receptors and channels were excluded as potential targets. Importantly, the pharmacological action of VSN16R was clearly blocked via BK_{Ca} antagonism and demonstrates that this is a new target to control spasticity.

This study indicates that potassium-induced hyperpolarisation following opening of the alpha pore in BK_{Ca} channels is a novel central mechanism of action of these drugs and in neural membranes will act to limit excessive action potential generation. Such membrane hyperpolarization is the common mechanism of action of many anti-spastic agents, which counter excitatory depolarizing signals that can lead to spasticity (Trompetto et al. 2014, Toda et al. 2014). This pathway is mediated directly via BK_{Ca} potassium channel opening, as shown here, and via calcium channel inhibition and notably activation of inwardly rectifying potassium channels after G protein signalling with CB_1R and $GABA_B$ agonists and through chloride ion influx following stimulation of $GABA_A$ receptors (Isomoto et al. 1997, Howlett et al. 2002, Pertwee et al. 2010). However, in contrast to cannabinoids and GABA agonists, VSN16R is well-tolerated in animals, even following direct injection into the brain. Likewise, BMS-204352, which is highly hydrophobic and readily enters the brain, also has a large therapeutic window in rodents (Gribkoff et al. 2001, Kristensen et al. 2011). As BK_{Ca} are activated in depolarizing conditions, it is possible that BK_{Ca} conformation targeted by VSN16R may only be active in certain states. As such it is of interest that NS-1619 fails to influence acute nociception but controls chronic neuropathic pain (Chen et al. 1997), suggesting that the BK_{Ca} targets may be pathologically expressed. This may contribute to the lack of sedating effects observed here in both animals and humans. As the first example of a neuronal-selective BK_{Ca} ligand, VSN16R may be the prototype for a new range of well-tolerated drugs with applications in diverse conditions in which excitotoxicity is evident or where the channel has a specific role. VSN16R was originally designed as a cyclic analogue of anandamide to exploit the benefit that the endocannabinoid system has to offer. Importantly however, it moves us away from the cannabis plant, and all its issues of recreational use, towards a novel pharmaceutical class of agents that offers therapeutic benefits without the psychoactive effects associated with cannabis use (Howlett et al. 2002, Varvel et al. 2005), or the sedating effects of other current anti-spastic agents (Shakespeare et al. 2003). This suggests that VSN16R is ready for testing in people with spasticity in MS (EudraCT 2014-004412-11, NCT02542787) to control neurological disease.

AUTHOR CONTRIBUTIONS.

Concept: DB, GP, DLS. Chemistry and compound design: CV, MO, DLS. Experimental Design: AIB; DB, DLS, GP, MDB, GG, JS, WSVH; RGP; Tissue based *in vitro* assays: AIB; AJI, CMH, CT; IS, LS, RR, SS, AJI, WSVH Production and management of mouse lines DB, GP, SS, SJJ; In vivo Assays: DB, GP, MDB, SA, SS, TEW; Phase I Trial development JS, KP, GG; Funding: AIB, DB, DLS, CV, GG, JS, KP, SJJ, WFG; Manuscript: All

ACKNOWLEDGEMENTS

The authors are grateful for the support of the Austrian science funds (FWF; P 27238), BioTechMed; Brain Research Trust, the Multiple Sclerosis Society, the Bloomsbury Bioseed Fund, Esparante Ventures, The Wellcome Trust, University College London Business, Fastforward USA, MS Ventures, Swiss Science Foundation grant (#310030_152578) and the Technology Strategy Board UK/Innovate UK.

CONFLICTS OF INTEREST

Some of the authors (DB, CV, GP, DLS) have filed patents based on the work within this study. DB, CV and DLS are founders and shareholders of Canbex Therapeutics Limited, a UCL spin-out company aiming to develop VSN16-related compounds. GP and GG are shareholders of Canbex Therapeutics JS and KP manage and are shareholders of Canbex Therapeutics and DB, GG and DLS are consultants to Canbex Therapeutics. The Institutions of AIB, AJI, DB, DLS, RGP, RR, WFG, WSVH received funds from Canbex Therapeutics to support VSN16R-related research.

REFERENCES

Alexander SPH, Kelly E, Marrion N, Peters JA, Benson HE, Faccenda E et al. (2015a) The Concise Guide to PHARMACOLOGY 2015/16: Overview. Br J Pharmacol. 172: 5729-5743.

Alexander SPH, Davenport AP, Kelly E, Marrion N, Peters JA, Benson HE, et al., (2015b) The Concise Guide to PHARMACOLOGY 2015/16: G protein-coupled receptors. Br J Pharmacol. 172: 5744-5869.

Alexander SPH, Peters JA, Kelly E, Marrion N, Benson HE, Faccenda E, et al. (2015c) The Concise Guide to PHARMACOLOGY 2015/16: Ligand-gated ion channels. Br J Pharmacol. 172: 5870-5903.

Al-Izki S, Pryce G, O'Neill JK, Butter C, Giovannoni G, Amor S et al. (2012) Practical guide to the induction of relapsing progressive experimental autoimmune encephalomyelitis in the Biozzi ABH mouse. Mult Scler Rel Dis. 1:29-28.

Al-Izki S, Pryce G, Hankey DJ, Lidster K, von Kutzleben SM, Browne L, et al. (2014) Lesional-targeting of neuroprotection to the inflammatory penumbra in experimental multiple sclerosis. Brain. 137:92-108.

Allen Brain Atlas. Mouse brain atlas, mouse spinal cord atlas. http://www.brain-map.org/

Baker D, Pryce G, Croxford JL, Brown P, Pertwee RG, Huffman JW et al. (2000) Cannabinoids control spasticity and tremor in a multiple sclerosis model. Nature. 404:84-87.

Baker D, Pryce G, Davies WL, Hiley CR (2006) In silico patent searching reveals a new cannabinoid receptor.Trends Pharmacol Sci. 27:1-4.

Baker D, Pryce G, Jackson SJ, Bolton C, Giovannoni G. (2012) The biology that underpins the therapeutic potential of cannabis-based medicines for the control of spasticity in multiple sclerosis. Mult Scler Rel Dis. 1:64-75

Barnes MP, Kent RM, Semlyen JK, McMullen KM. (2003) Spasticity in multiple sclerosis. Neurorehabil Neural Repair. 17:66-70.

Bednarczyk P, Koziel A, Jarmuszkiewicz W, Szewczyk A. (2013) Large-conductance Ca^{2+}-activated potassium channel in mitochondria of endothelial EA.hy926 cells. Am J Physiol Heart Circ Physiol. 304:H1415-427

Begg M, Mo FM, Offertaler L, Bátkai S, Pacher P, Razdan RK et al. (2003). G protein-coupled endothelial receptor for atypical cannabinoid ligands modulates a Ca2+-dependent K+ current. J Biol Chem. 278: 46188-46194.

Berglund BA, Fleming PR, Rice KC, Shim JY, Welsh WJ, Howlett AC. (2000) Development of a novel class of monocyclic and bicyclic alkyl amides that exhibit CB1 and CB2 cannabinoid receptor affinity and receptor activation. Drug Des Discov. 16:281-294.

Bondarenko AI, Malli R, Graier WF. (2011) The GPR55 agonist lysophosphatidylinositol acts as an intracellular messenger and bidirectionally modulates Ca2+ -activated large-conductance K+ channels in endothelial cells. Pflugers Arch. 461:177-189.

Bondarenko AI, Drachuk K, Panasiuk O, Sagach V, Deak AT, Malli R et al. (2013) N-arachidonoyl glycine suppresses Na^{+}/Ca^{2+} exchanger-mediated Ca^{2+} entry into endothelial cells and activates BK channels independently of G-protein coupled receptors. Br J Pharmacol 169: 933-948.

Bondarenko AI. (2014) Endothelial atypical cannabinoid receptor: do we have enough evidence? Br J Pharmacol. 171:5573-5588.

Brenner R, Perez GJ, Bonev AD, Eckman DM, Kosek JC, Wiler SW et al. (2000) Vasoregulation by the beta1 subunit of the calcium-activated potassium channel. Nature 407:870-876.

Brenner R, Chen QH, Vilaythong A, Toney GM, Noebels JL, Aldrich RW. (2005) BK channel beta4 subunit reduces dentate gyrus excitability and protects against temporal lobe seizures. Nat Neurosci.8: 1752-1759.

Burnstock G, Verkhratsky A. (2010) Vas deferens--a model used to establish sympathetic cotransmission. Trends Pharmacol Sci. 31:131-139.

Chen SR, Cai YQ, Pan HL. (2009) Plasticity and emerging role of BKCa channels in nociceptive control in neuropathic pain J Neurochem. 110:352-362.

Compston A, Coles A. (2002) Multiple sclerosis. Lancet. 359:1221-1231.

Curtis MJ, Bond RA, Spina D, Ahluwalia A, Alexander SP, Giembycz MA et al. Experimental design and analysis and their reporting: new guidance for publication in BJP. Br J Pharmacol. 2015; 172:3461-3471.

Freeman TC, , Dixon AK, Campbell EA, Tait TM, Richardson PJ, Rice KM, et al. (1998) Expression mapping of mouse genes. MGI Direct Data Submission J:46439.

Godlewski G, Offertáler L, Osei-Hyiaman D, Mo FM, Harvey-White J, Liu J et al. (2009) The endogenous brain constituent N-arachidonoyl L-serine is an activator of large conductance Ca2+-activated K+ channels. J Pharmacol Exp Ther. 2009; 328 : 351-361.

Gessner G, Cui YM, Otani Y, Ohwada T, Soom M, Hoshi T et al. (2012) Molecular mechanism of pharmacological activation of BK channels. Proc. Natl. Acad. Sci. U.S.A. 109, 3552–3557.

Gribkoff VK, Starrett JE Jr, Dworetzky SI, Hewawasam P, Boissard CG, Cook DA et al. (2001) Targeting acute ischemic stroke with a calcium-sensitive opener of maxi-K potassium channels. Nat Med. 7:471-477.

Hilliard A, Stott C, Wright S, Guy G, Pryce G, Al-Izki S et al. (2012) Evaluation of the Effects of Sativex (THC BDS: CBD BDS) on Inhibition of Spasticity in a Chronic Relapsing Experimental Allergic Autoimmune Encephalomyelitis: A Model of Multiple Sclerosis. ISRN Neurol. 2012:802649

Ho WS, Randall MD. (2007) Endothelium-dependent metabolism by endocannabinoid hydrolases and cyclooxygenases limits vasorelaxation to anandamide and 2-arachidonoylglycerol. Br J Pharmacol. 150:641-651.

Hoi PM, Visintin C, Okuyama M, Gardiner SM, Kaup SS, Bennett T, et al. (2007) Vascular pharmacology of a novel cannabinoid-like compound, 3-(5-dimethylcarbamoyl-pent-1-enyl)-N-(2-hydroxy-1-methyl-ethyl)benzamide (VSN16) in the rat. Br J Pharmacol. 152:751-764.

Howlett AC, Barth F, Bonner TI, Cabral G, Casellas P, Devane WA et al (20002) International Union of Pharmacology. XXVII. Classification of cannabinoid receptors. Pharmacol Rev. 54:161-202.

Imlach WL, Finch SC, Dunlop J, Meredith AL, Aldrich RW, Dalziel JE. (2008) The molecular mechanism of "ryegrass staggers," a neurological disorder of K+ channels.J Pharmacol Exp Ther. 327:657-664.

Isomoto S, Kondo C, Kurachi Y. (1997) Inwardly rectifying potassium channels: their molecular heterogeneity and function. Jpn J Physiol. 47:11-39.

Jin P, weiger TM, Levian IB. (2002) Reciprocal Modulation between the alpha and beta4 Subunits of h*Slo* calcium-dependent potassium channels. J. Biol Chem. 272:43724-43729.

Kristensen LV, Sandager-Nielsen K, Hansen HH. (2011) Kv7 (KCNQ) channel openers induce hypothermia in the mouse. Neurosci Lett. 488:178-182.

Leocani L, Nuara A, Houdayer E, Schiavetti I, Del Carro U, Amadio S et al. (2015) Sativex and clinical-neurophysiological measures of spasticity in progressive multiple sclerosis. J Neurol. 262: 2520-2527.

Li Y, Gorassini MA, Bennett DJ. (2004) Role of persistent sodium and calcium currents in motoneuron firing and spasticity in chronic spinal rats. J Neurophysiol. 91:767-783.

Liu CY, Lu ZY, Li N, Yu LH, Zhao YF, Ma B. (2015). The role of large-conductance, calcium-activated potassium channels in a rat model of trigeminal neuropathic pain. Cephalalgia. 35:16-35.

Martinez-Espinosa PL, Yang C, Gonzalez-Perez V, Xia XM, Lingle CJ. (2014) Knockout of the BK beta2 subunit abolishes inactivation of BK currents in mouse adrenal chromaffin cells and results in slow-wave burst activity. J Gen Physiol. 4: 275-295

Matthews WB. (1966) Ratio of maximum H reflex to maximum M response as a measure of spasticity J Neurol Neurosurg Psychiatry. 29: 201–204.

Modol L, Mancuso R, Alé A, Francos-Quijorna I, Navarro X. (2014) Differential effects of KCC2 expression and spasticity of ALS and traumatic injuries to motoneurons. Front Cell Neurosci 8:7.

McHugh D, Hu SS, Rimmerman N, Juknat A, Vogel Z, Walker JM et al. (2010) N-arachidonoyl glycine, in abundant endogenous lipid, potentially drives directed cellular migration through GPR18, the putative abnormal cannabidiol receptor. BMC Neurosci 11:44.

N'Gouemo P (2014). BKCa channel dysfunction in neurological diseases. Front Physiol. 5:373.

Novotna A, Mares J, Ratcliffe S, Novakova I, Vachova M, Zapletalova O et al. (2011) A randomized, double-blind, placebo-controlled, parallel-group, enriched-design study of nabiximols* (Sativex), as add-on therapy, in subjects with refractory spasticity caused by multiple sclerosis. Eur J Neurol. 18:1122-1131.

Papassotiriou J, Köhler R, Prenen J, Krause H, Akbar M, Eggermont J, et al. (2000) Endothelial K(+) channel lacks the Ca(2+) sensitivity-regulating beta subunit. FASEB J. 14:885-894.

Pertwee RG, Howlett AC, Abood ME, Alexander SP, Di Marzo V, Elphick MR et al.(2010) International Union of Basic and Clinical Pharmacology. LXXIX. Cannabinoid receptors and their ligands: beyond CB1 and CB2. Pharmacol Rev. 62:588-631.

Parmar N, Ho WS (2010). N-arachidonoyl glycine, an endogenous lipid that acts as a vasorelaxant via nitric oxide and large conductance calcium-activated potassium channels. Br J Pharmacol ; 160: 594-603.

Pryce G, Ahmed Z, Hankey DJ, Jackson SJ, Croxford JL, Pocock JM et al. (2013) Cannabinoids inhibit neurodegeneration in models of multiple sclerosis. Brain. 2003; 126:2191-2202.

Pryce G, Visintin C, Ramagopalan SV, Al-Izki S, De Faveri LE, Nuamah RA et al. (2014). Control of spasticity in a multiple sclerosis model using central nervous system-excluded CB1 cannabinoid receptor agonists. FASEB J. 28:117-130.

Ross RA, Gibson TM, Brockie HC, Leslie M, Pashmi G, Craib SJ et al. (2001) Structure-activity relationship for the endogenous cannabinoid, anandamide, and certain of its analogues at vanilloid receptors in transfected cells and vas deferens. Br J Pharmacol. 132:631-640.

Roux S, Sable E, Porsolt RD (2005). Primary observation (Irwin) test in rodents for assessing acute toxicity of a test agent and its effects on behavior and physiological function. Curr Protoc Pharmacol. Chapter 10:Unit 10.10.

Sánchez-Pastor E, Andrade F, Sánchez-Pastor JM, Elizalde A, Huerta M, Virgen-Ortiz A et al. (2014). Cannabinoid receptor type 1 activation by arachidonylcyclopropylamide in rat aortic rings causes vasorelaxation involving calcium-activated potassium channel subunit alpha-1 and calcium channel, voltage-dependent, L type, alpha 1C subunit. Eur J Pharmacol. 729: 100-106.

Sausbier M, Hu H, Arntz C, Feil S, Kamm S, Adelsberger H et al. (2004). Cerebellar ataxia and Purkinje cell dysfunction caused by Ca2+-activated K+ channel deficiency. Proc Natl Acad Sci U S A. 2004; 101:9474-9478.

Sevastou I, Pryce G, Baker D, Selwood DL. (2016). Characterisation of Transcriptional Changes in the Spinal Cord of the Progressive Experimental Autoimmune Encephalomyelitis Biozzi ABH Mouse Model by RNA Sequencing. PLoS One. 11(6):e0157754.

Shakespeare DT, Boggild M, Young C. (2003). Anti-spasticity agents for multiple sclerosis. Cochrane Database Syst Rev. (4):CD001332.

Sisay S, Pryce G, Jackson SJ, Tanner C, Ross RA, Michael GJ et al. (2013) Genetic background can result in a marked or minimal effect of gene knockout (GPR55 and CB2 receptor) in experimental autoimmune encephalomyelitis models of multiple sclerosis. PLoS One. 8:e76907.

Southan C, Sharman JL, Benson HE, Faccenda E, Pawson AJ, Alexander SP *et al.* (2016). The IUPHAR/BPS Guide to PHARMACOLOGY in 2016: towards curated quantitative interactions between 1300 protein targets and 6000 ligands. Nucl Acids Res 44: D1054-1068

Toda T, Ishida K, Kiyama H, Yamashita T, Lee S. (2014) Down-regulation of KCC2 expression and phosphorylation in motoneurons, and increases the number of in primary afferent projections to motoneurons in mice with post-stroke spasticity. PLoS One. 9:e114328.

Trompetto C, Marinelli L, Mori L, Pelosin E, Currà A, Molfetta L, Abbruzzese G. (2014) Pathophysiology of spasticity: implications for neurorehabilitation. Biomed Res Int. 2014:354906.

Varvel SA, Bridgen DT, Tao Q, Thomas BF, Martin BR, Lichtman AH. (2005) Delta9-tetrahydrocannbinol accounts for the antinociceptive, hypothermic, and cataleptic effects of marijuana in mice. J Pharmacol Exp Ther. 314:329-37

Weiger TM. Holmqvist MH, Levitan IB, Clark FT, Sprague S, Huang WJ et al. (2000) A novel nervous system beta subunit that downregulates human large conductance calcium-dependent potassium channels. J Neurosci. 20:3563-3570.

White R, Hiley CR. (1998) The actions of the cannabinoid receptor antagonist, SR 141716A, in the rat isolated mesenteric artery. Br J Pharmacol. 125:689-696.

Wininger M, Craelius W, Settle J, Robinson S, Isaac B, Maloni H et al.(2015). Biomechanical analysis of spasticity-treatment in patients with multiple sclerosis. Ther Adv Neurol Disord. 8:203-211.

Zhang J, Yan J Regulation of BK channels by auxiliary γ subunits. (2014) Front Physiol. 5: 401.

Xie J, McCobb DP. (1998) Control of alternative splicing of potassium channels by stress hormones. Science. 280:443-446.

Zheng YM, Park SW, Stokes L, Tang Q, Xiao JH, Wang YX. Distinct activity of BK channel β1-subunit in cerebral and pulmonary artery smooth muscle cells. Am J Physiol Cell Physiol. 2013 304:C780-789.

FIGURE LEGENDS

FIGURE 1

VSN16 inhibits spasticity without sedation. (A, B). Inhibition of electrically evoked contraction of the mouse vas deferens following incubation with various doses of (A) VSN16 with or without pre-incubation of 31.6nM SR141617A, (B) R(+)WIN55,212. n=5-6 replicates. (C, D) Lack of sedative effect of 1mg/kg VSN16 in ABH mice compared with 1mg/kg R(+)WIN55,212 (n=5) or 5mg/kg i.v. baclofen (n=4). The results represent the mean ± SEM. (C) hypomotility in a 27 x 27cm open field chamber 30min after intravenous drug administration and (D) Hypothermia 20min after drug administration via the i.v. or intracerebral (i.c.) route in wildtype ABH mice or CB_1R-deficient mice (n=4 animals/group) except baclofen (n=10 animals).(E) Inhibition of spasticity measured as the resistance to hindlimb flexion against a strain gauge in visibly spastic ABH mice, showing mean± SEM following Injection of 1mg/kg i.v. VSN16 racemate. n=6 animals n=9 limbs. * significantly different compared to baseline. VSN16 structure in the insert with chiral center (*) indicated (F) Pharmacokinetics of VSN16R in outbred mice and rats following intravenous or oral administration mean ± SEM. n=3 male animals/group (G, H) Inhibition of spasticity measured as the resistance to hindlimb flexion against a strain gauge in visibly spastic ABH mice, showing mean ± SEM (G) 5mg/kg i.v. VSN16R (n=7 animals, n=14 limbs) or VSN16S (n=7 animals, n=13 limbs). (H) Percentage changed in resistance to hindlimb flexion from baseline following vehicle (n=8 animals. n=14 limbs), 5mg/kg i.v. VSN16R (n=7 animals, n=14 limbs), 5mg/kg i.v. baclofen (n=6 animals. n=10 limbs) or 5mg/kg i.v. (n=8 animals. n=13 limbs) or 10mg/kg i.v. (n=6 animals. n=11 limbs) using botanical drug substances within medicinal cannabis (Hilliard et al. 2012). These were undertaken as separate experiments. * significantly different compared to baseline.

FIGURE 2. *Oral VSN16R inhibits spasticity* Inhibition of spasticity measured as the resistance to flexion against a strain gauge in visibly spastic ABH mice showing mean± SEM force requires for flexion. Animals received oral (A) 0.5mg/kg (n=10 animals. n=20 limbs, 1mg/kg (n=10 animals n=18 limbs. $P<0.001$) or 5mg/kg p.o. VSN16R in water (n=10 animals. n=19 limbs) (B) The change in resistance to flexion forces of individual limbs from baseline to 60min following 5mg/kg p.o. administration (n=17 animals. n= 32 limbs). (C) 40mg/kg VSN16R (n=8 animals, n=15 limbs) (D) Repeated daily administration of 40mg/kg with measurement on the first and eight day of treatment (n=8 animals n=15 limbs). (E) Repeated daily administration of vehicle (n=9. n=18 limbs) or 5 mg/kg p.o. in baclofen in water (n=7 animals. n=14 limbs), where there was no difference at baseline between day 0 and 7. (E) Repeated daily 25mg/kg CNQX subcutaneous (n=5 animals, n=10 limbs). * significantly different compared to baseline. (F) Comparison of 5mg/kg p.o. VSN16R in water (n=17 animals) and vehicle treated animals (n=17

animals) using a single mean combined from both limbs, rather than analysis of individual limbs. # significantly different compared to vehicle treated animals. (F) Plasma levels of VSN16R following oral delivery of 5mg/kg VSN16R to spastic ABH mice with EAE or 400mg VSN16R (~5mg/kg) p.o. in healthy humans n=6.

FIGURE 3.

VSN16R produces active metabolites. (A) VSN16R was incubated with primary mouse rat, monkey and human hepatocytes and 1h later the supernatants were assessed by liquid crystallography mass spectroscopy and two species, VSN22R and VSN44R, were identified and the results expressed as percentage of the original starting material. Insert shows the structure of VSN22R and VSN44R (B) Inhibition of electrically evoked contraction of the mouse vas deferens following incubation with various doses of VSN22R and VSN44R (n=5 replicates) (C) VSN16R (n=8 cultured), VSN22R (n=6 cultures), VSN44R (n=8 cultures)-mediated relaxation of methoxamine-evoked contraction in rat mesenteric arteries. (D) Inhibition of spasticity measured as the resistance to hindlimb flexion against a strain gauge in visibly spastic ABH mice, showing mean ± SEM following injection of 5mg/kg i.v. VSN16R (n=7 animals. n=14 limbs), VSN22R (n=7 animals. n=14 limbs) or VSN44R (n=9 animals. n=18 limbs). * significantly different compared to baseline.

FIGURE 4.

Pharmacokinetics of VSN16R in rats, dogs and humans. Liquid chromatography mass spectrometry plasma levels of detecting VSN16R, VSN22R or VSN44R in (A) Rat after 5mg/kg or 50mg/kg VSN16R p.o. n=6/group (B) Dogs after 50mg/kg p.o. (n=6) (C) Human VSN16R levels after 25mg, 50mg, 100mg. 200mg, 400mg and 800mg (D) Human VSN16R, VSN22R and VSN44R levels after 25mg and 800mg VSN16R p.o. n=6 subjects/group (E) Human VSN16R, VSN22R and VSN44R plasma levels after twice daily 400mg VSN16R p.o., where the twelve hour sample was taken immediately before dosing n=6 humans/group and (F) Human VSN16R, VSN22R and VSN44R plasma levels after 200mg VSN16R p.o. in people that were fed or fasted before drug administration.

FIGURE 5.

VSN16R is a BK_{Ca} opener. (A) Percentage change in resistance to flexion in response to treatment with either 1mg/kg i.p. CP55,950 (n=5 animals, n=8 limbs), 5mg/kg i.p. R(+)WIN55,212 (n=7 animals. n=14 limbs) or 5mg/kg i.v. VSN16R in wildtype ABH (n=7 animals, n=14 limbs) or congenic CB_1R deficient mice (n=5 animals/ group n=10 limbs) at 30min after treatment (B) Change in resistance to flexion in response to treatment with vehicle (n=8 animals. n=14 limbs) or 10mg/kg i.v. VSN16R wildtype ABH (n=

8 animals. n=16 limbs) or congenic GPR55-deficient mice (n=8 animals. n=15 limbs) (C, D) VSN16R-mediated relaxation of methoxamine-evoked contraction in rat mesenteric arteries in a dose-response to VSN16. (C) Endothelial intact (n=11 assays), endothelium denuded (n=6 assays) or endothelium intact cultures in the presence of 60mM KCl (n=4 assays). (D) Vehicle-treated controls (n=17 assays) or pretreated with 50nM apamin (n=7 assays), 50nM iberotoxin (n=5 assays), 50nM charybdotoxin (n=6 assays) or a combination of apamin and charybdotoxin (n=6 assays). (E) 3 μM VSN16R, VSN22R and VSN44R stimulate single BK_{Ca} channel activity in excised from EA.hy926 cells inside-out patches held at 40 mV and exposed to 0.3 μM free Ca^{2+} representative plots (F-G) Statistical representation of the potentiation of BK_{Ca} single channel activity (*N*Po) by 3 μM VSN16R at (F) concentration-dependent increase in *N*Po by 0.3-30 μM VSN16R at a holding voltage 60 mV and (G) different voltages and fixed Ca^{2+} 300 nM. The number of patches is shown in brackets. The results represent the mean ± SD. (H) VSN16R stimulates single BK_{Ca} channel activity in inside-out patch excised from human neural HCN-2 cells and held at either 20mV or 40mv in the presence of 0.3 μM free Ca^{2+} (n=4 patches).

FIGURE 6

***BK_{Ca} openers control spasticity*.** (A) RNAseq expression of BK_{Ca} channel components in EA.hy926 cells. Insert represents the western blot of KCNMB4 in EA.hy926 cells, which was tested in 4 samples, and Western blot of KCNMB4 expression in the spinal cord in control (n=3) and spastic EAE spinal cord tissues (2 shown. n=6 total) showing an additional prominent band, not present in EA.hy926 cells, above the anticipated fragment size more notable during EAE. This antibody detected multiple bands in western analysis (B) RNAseq expression of BK_{Ca} channel components in the spinal cords of spastic EAE (n=3mice) and age-matched normal mice (n=3 mice). The results represent the mean ± SEM. Insert represents the western blot of KCNMA1 in control and spastic EAE tissue (Antibody APC-021 detected a single band at the anticipated size and was repeated with antibody APC-151 with comparable results) and inserts shows a significant change in ratio between *Kcnma1* and Neurofilament light (*Nefl*) gene levels. (C) Percentage change in resistance to flexion of spastic hindlimbs in ABH mice in response to treatment with 5mg/kg p.o. VSN16R in water (n=10 animals. n=19 limbs) that were pretreated with saline or 1mg/kg i.p. paxilline (n=7animals. n=14 limbs) (D) percentage change in resistance to flexion of hindlimbs in ABH mice following injection i.p. with 1mg/kg paxilline (n=7 animals. n=13 limbs. p=0.061), 40mg/kg i.p. BMS-204352 (n=7 animals. n= 13 limbs); 20mg/kg i.p. NS-1619 (n=7 animals. n=14 limbs), or 10mg/kg i.p. NS-11021 (n=7 animals. n=13 limbs). * Significant difference compared to baseline.

FIGURE 1

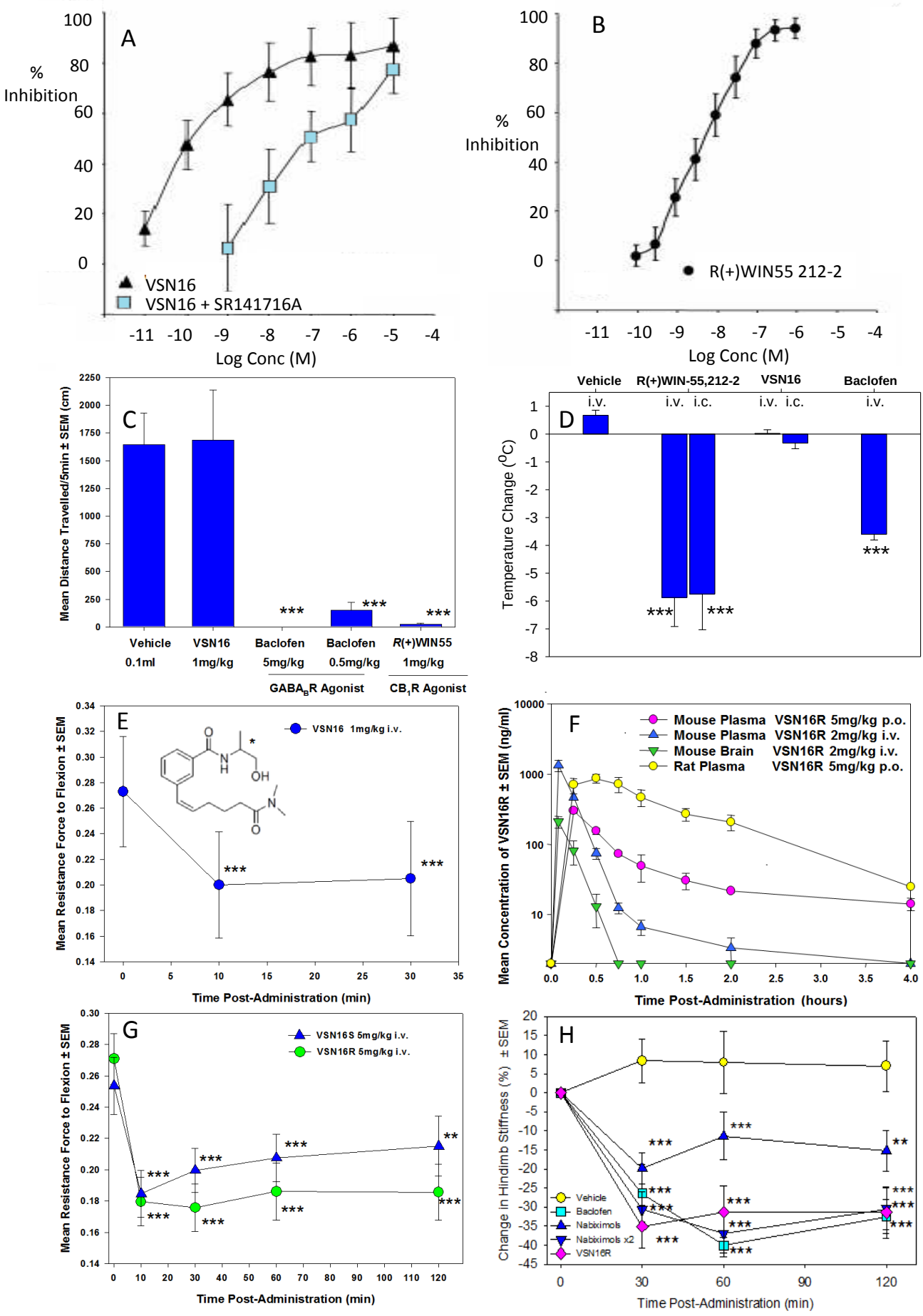
A
% Inhibition
VSN16
VSN16 + SR141716A
Log Conc (M)
B
% Inhibition
R(+)WIN55 212-2
Log Conc (M)
C
Mean Distance Travelled/5min ± SEM (cm)
Vehicle 0.1ml
VSN16 1mg/kg
Baclofen 5mg/kg
Baclofen 0.5mg/kg
R(+)WIN55 1mg/kg
GABA$_B$R Agonist
CB$_1$R Agonist
D
Vehicle
R(+)WIN-55,212-2
VSN16
Baclofen
i.v.
i.c.
Temperature Change (°C)
E
VSN16 1mg/kg i.v.
Mean Resistance Force to Flexion ± SEM
Time Post-Administration (min)
F
Mouse Plasma VSN16R 5mg/kg p.o.
Mouse Plasma VSN16R 2mg/kg i.v.
Mouse Brain VSN16R 2mg/kg i.v.
Rat Plasma VSN16R 5mg/kg p.o.
Mean Concentration of VSN16R ± SEM (ng/ml)
Time Post-Administration (hours)
G
VSN16S 5mg/kg i.v.
VSN16R 5mg/kg i.v.
Mean Resistance Force to Flexion ± SEM
Time Post-Administration (min)
H
Vehicle
Baclofen
Nabiximols
Nabiximols x2
VSN16R
Change in Hindlimb Stiffness (%) ± SEM
Time Post-Administration (min)

FIGURE 2

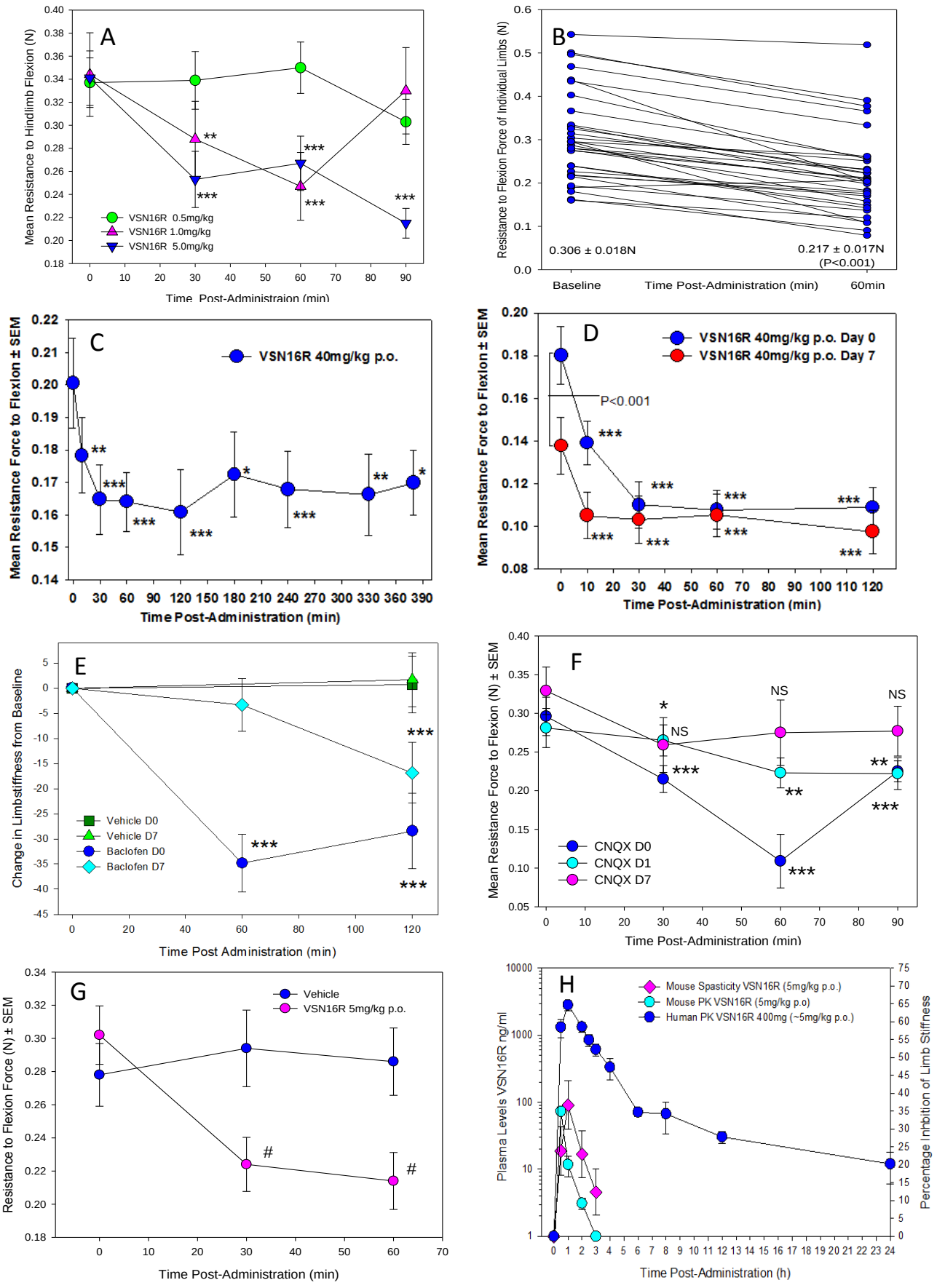
A
Mean Resistance to Hindlimb Flexion (N)
VSN16R 0.5mg/kg
VSN16R 1.0mg/kg
VSN16R 5.0mg/kg
Time Post-Administraion (min)
B
Resistance to Flexion Force of Individual Limbs (N)
0.306 ± 0.018N
0.217 ± 0.017N
(P<0.001)
Baseline
Time Post-Administration (min)
60min
C
VSN16R 40mg/kg p.o.
Mean Resistance Force to Flexion ± SEM
Time Post-Administration (min)
D
VSN16R 40mg/kg p.o. Day 0
VSN16R 40mg/kg p.o. Day 7
P<0.001
Mean Resistance Force to Flexion ± SEM
Time Post-Administration (min)
E
Change in Limbstiffness from Baseline
Vehicle D0
Vehicle D7
Baclofen D0
Baclofen D7
Time Post Administration (min)
F
Mean Resistance Force to Flexion (N) ± SEM
CNQX D0
CNQX D1
CNQX D7
NS
Time Post-Administration (min)
G
Vehicle
VSN16R 5mg/kg p.o.
Resistance to Flexion Force (N) ± SEM
Time Post-Administration (min)
H
Mouse Spasticity VSN16R (5mg/kg p.o.)
Mouse PK VSN16R (5mg/kg p.o)
Human PK VSN16R 400mg (~5mg/kg p.o.)
Plasma Levels VSN16R ng/ml
Percentage Inhibition of Limb Stiffness
Time Post-Administration (h)

FIGURE 3

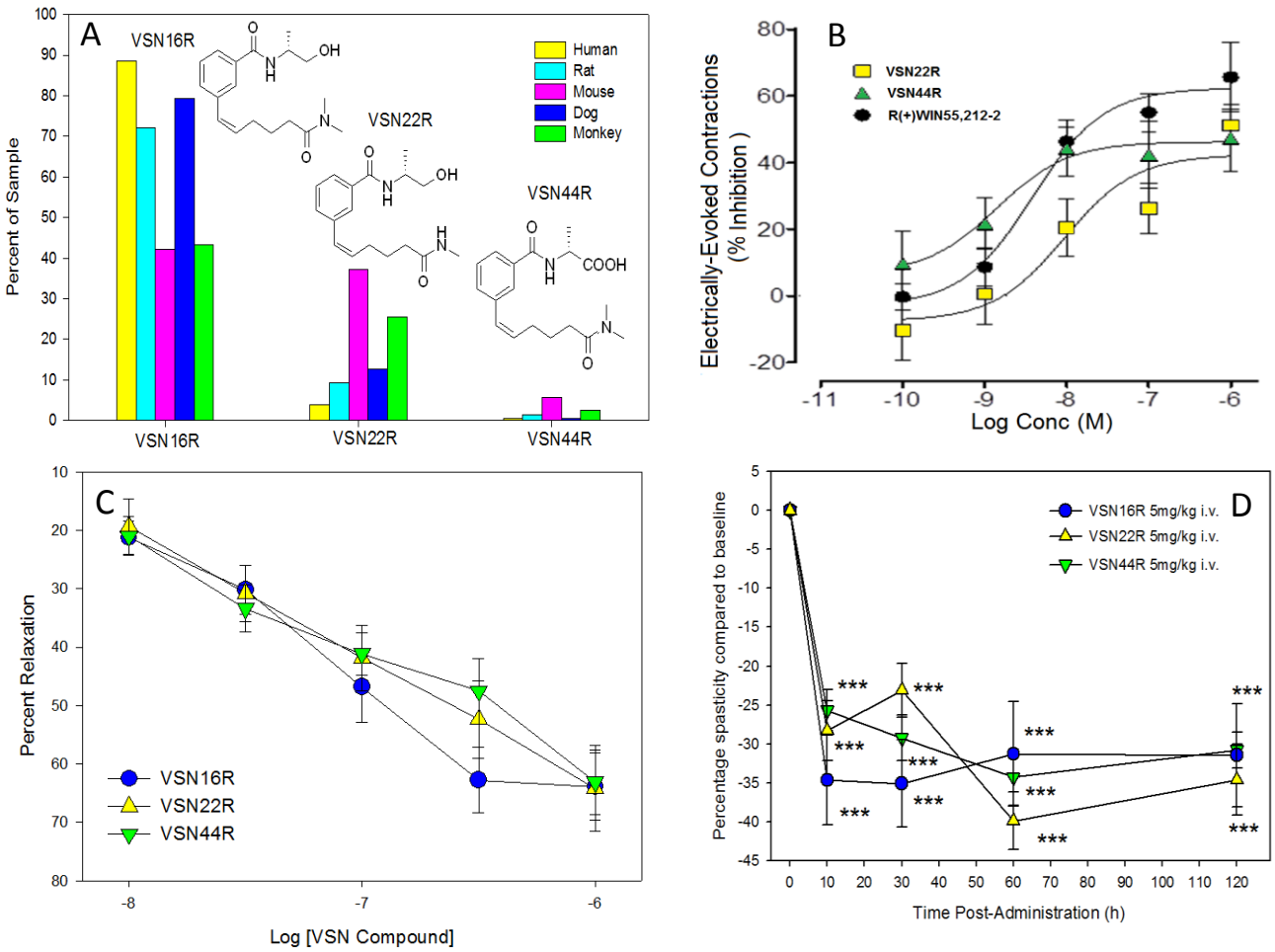
A
VSN16R
VSN22R
VSN44R
Human
Rat
Mouse
Dog
Monkey
Percent of Sample
B
VSN22R
VSN44R
R(+)WIN55,212-2
Electrically-Evoked Contractions (% Inhibition)
Log Conc (M)
C
VSN16R
VSN22R
VSN44R
Percent Relaxation
Log [VSN Compound]
D
VSN16R 5mg/kg i.v.
VSN22R 5mg/kg i.v.
VSN44R 5mg/kg i.v.
Percentage spasticity compared to baseline
Time Post-Administration (h)

FIGURE 4

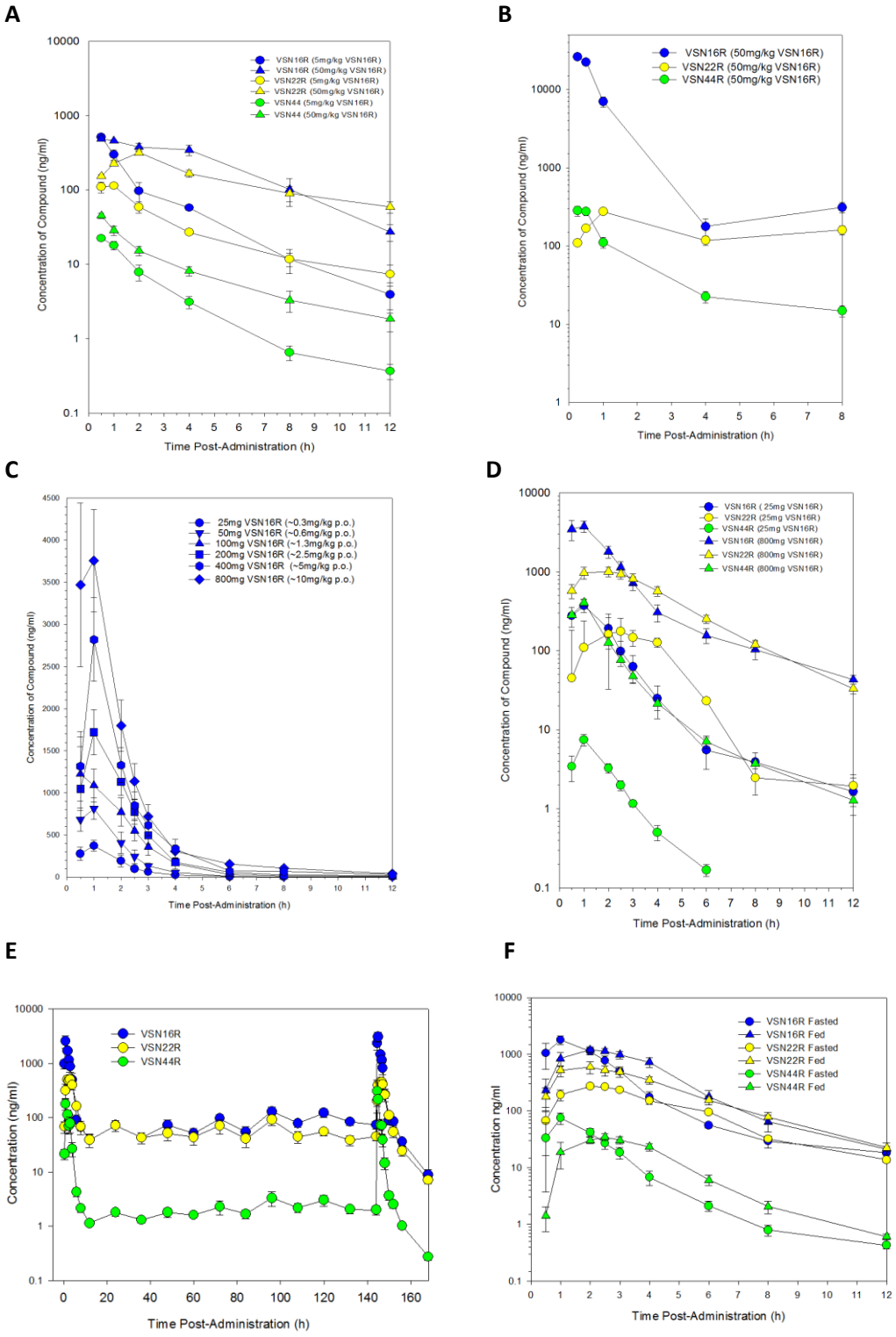
A
VSN16R (5mg/kg VSN16R)
VSN16R (50mg/kg VSN16R)
VSN22R (5mg/kg VSN16R)
VSN22R (50mg/kg VSN16R)
VSN44 (5mg/kg VSN16R)
VSN44 (50mg/kg VSN16R)
Concentration of Compound (ng/ml)
Time Post-Administration (h)
B
VSN16R (50mg/kg VSN16R)
VSN22R (50mg/kg VSN16R)
VSN44R (50mg/kg VSN16R)
Concentration of Compound (ng/ml)
Time Post-Administration (h)
C
25mg VSN16R (~0.3mg/kg p.o.)
50mg VSN16R (~0.6mg/kg p.o.)
100mg VSN16R (~1.3mg/kg p.o.)
200mg VSN16R (~2.5mg/kg p.o.)
400mg VSN16R (~5mg/kg p.o.)
800mg VSN16R (~10mg/kg p.o.)
Concentration of Compound (ng/ml)
Time Post-Administration (h)
D
VSN16R (25mg VSN16R)
VSN22R (25mg VSN16R)
VSN44R (25mg VSN16R)
VSN16R (800mg VSN16R)
VSN22R (800mg VSN16R)
VSN44R (800mg VSN16R)
Concentration of Compound (ng/ml)
Time Post-Administration (h)
E
VSN16R
VSN22R
VSN44R
Concentration (ng/ml)
Time Post-Administration (h)
F
VSN16R Fasted
VSN16R Fed
VSN22R Fasted
VSN22R Fed
VSN44R Fasted
VSN44R Fed
Concentration ng/ml
Time Post-Administration (h)

FIGURE 5

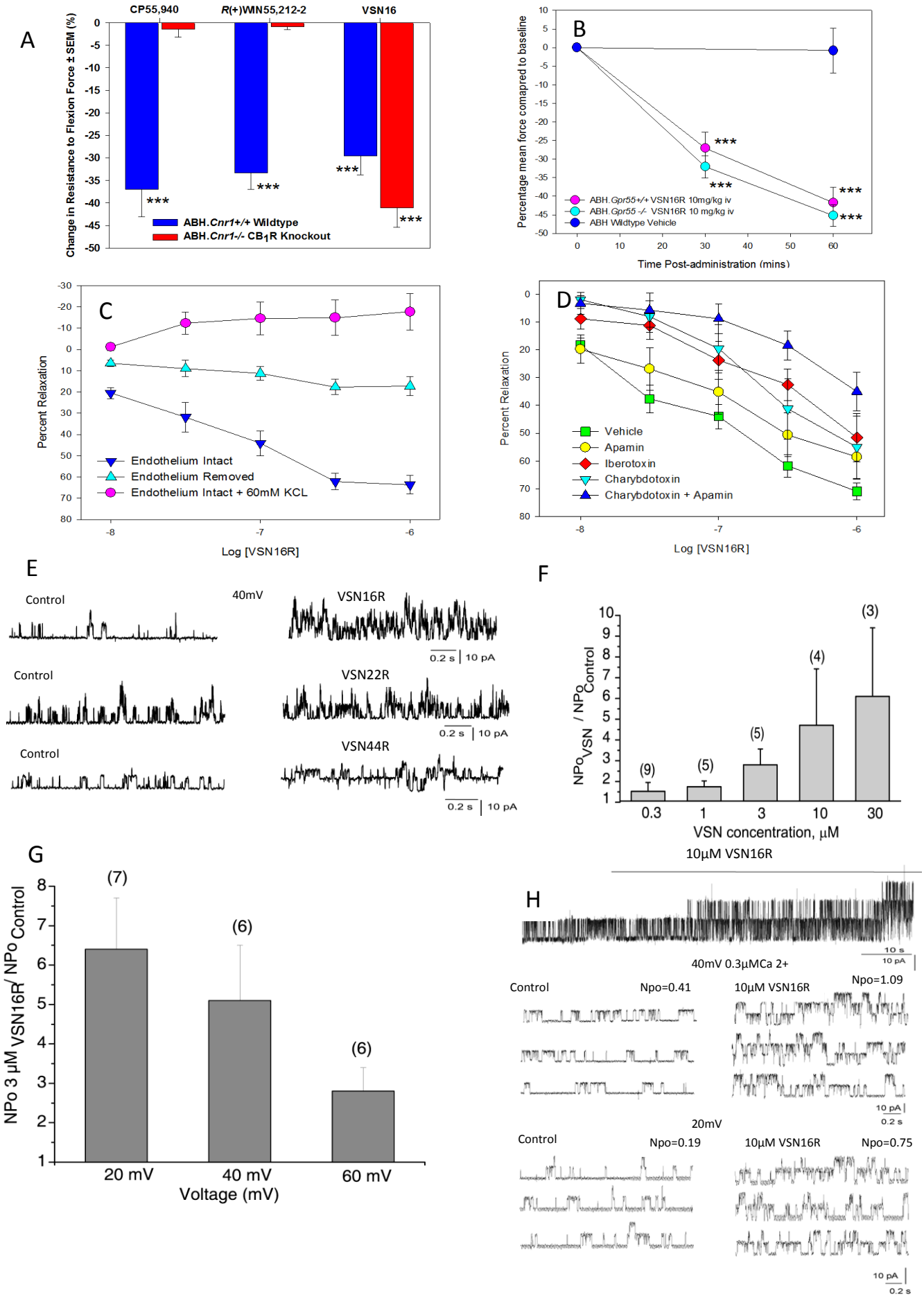
A
CP55,940
R(+)WIN55,212-2
VSN16
Change in Resistance to Flexion Force ± SEM (%)
ABH.Cnr1+/+ Wildtype
ABH.Cnr1-/- CB1R Knockout
***
B
Percentage mean force comapred to baseline
Time Post-administration (mins)
ABH.Gpr55+/+ VSN16R 10mg/kg iv
ABH.Gpr55 -/- VSN16R 10 mg/kg iv
ABH Wildtype Vehicle
C
Percent Relaxation
Log [VSN16R]
Endothelium Intact
Endothelium Removed
Endothelium Intact + 60mM KCL
D
Percent Relaxation
Log [VSN16R]
Vehicle
Apamin
Iberotoxin
Charybdotoxin
Charybdotoxin + Apamin
E
Control
40mV
VSN16R
VSN22R
VSN44R
0.2 s | 10 pA
F
NPo VSN / NPo Control
VSN concentration, µM
(9)
(5)
(3)
(4)
(5)
G
NPo 3 µM VSN16R/ NPo Control
Voltage (mV)
20 mV
40 mV
60 mV
(7)
(6)
(6)
H
10µM VSN16R
40mV 0.3µMCa 2+
Control
Npo=0.41
10µM VSN16R
Npo=1.09
20mV
Control
Npo=0.19
10µM VSN16R
Npo=0.75
10 pA
0.2 s

FIGURE 6

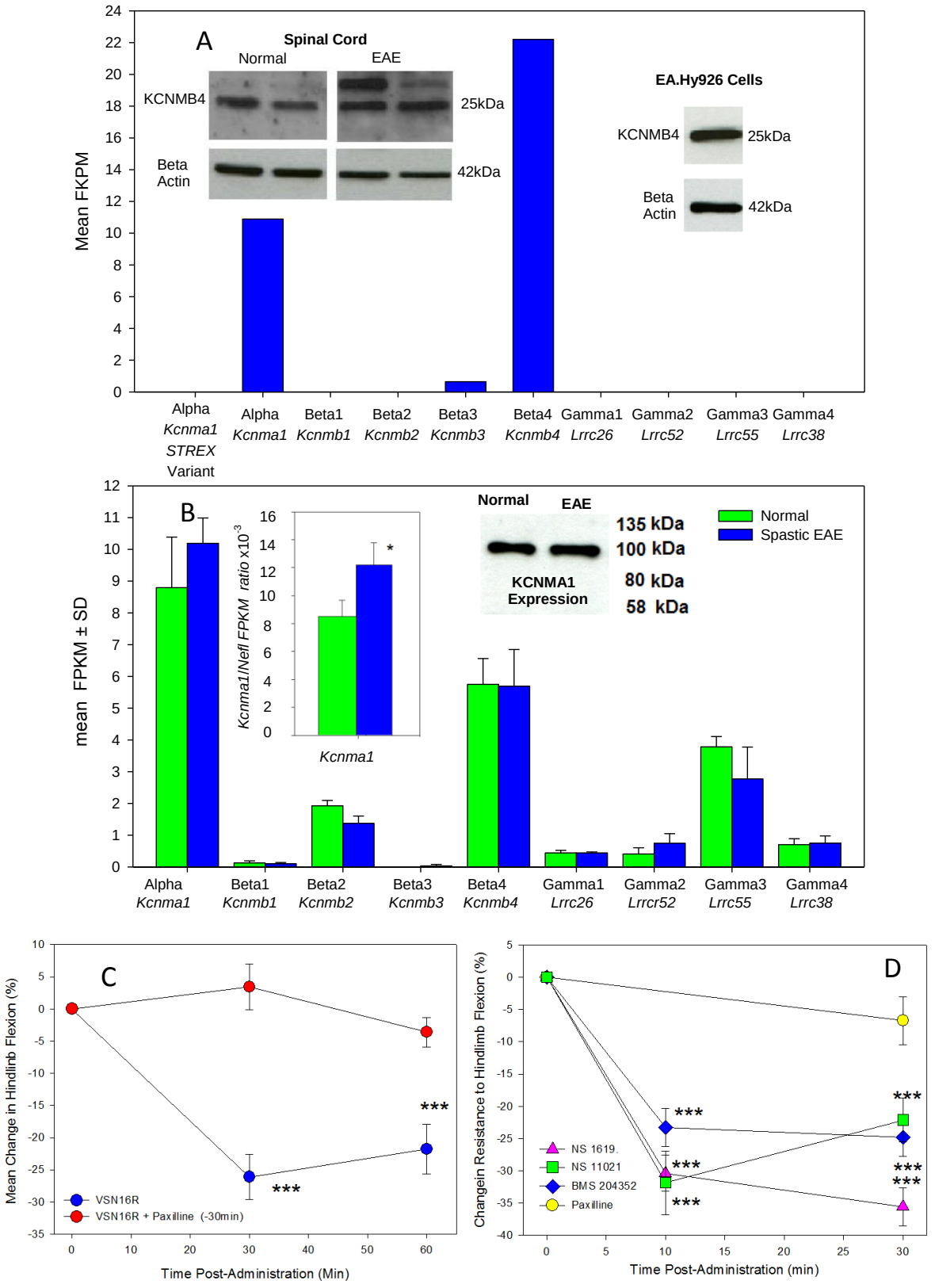
A
Spinal Cord
Normal
EAE
KCNMB4
25kDa
Beta Actin
42kDa
EA.Hy926 Cells
KCNMB4
25kDa
Beta Actin
42kDa
Mean FKPM
Alpha Kcnma1 STREX Variant
Alpha Kcnma1
Beta1 Kcnmb1
Beta2 Kcnmb2
Beta3 Kcnmb3
Beta4 Kcnmb4
Gamma1 Lrrc26
Gamma2 Lrrc52
Gamma3 Lrrc55
Gamma4 Lrrc38
B
Normal
EAE
135 kDa
100 kDa
80 kDa
58 kDa
KCNMA1 Expression
Normal
Spastic EAE
mean FPKM ± SD
Kcnma1/Nefl FPKM ratio x10-3
Kcnma1
C
Mean Change in Hindlimb Flexion (%)
VSN16R
VSN16R + Paxilline (-30min)
Time Post-Administration (Min)
D
Changein Resistance to Hindlimb Flexion (%)
NS 1619.
NS 11021
BMS 204352
Paxilline
Time Post-Administration (min)

SUPPLEMENTARY MATERIAL

METHODS 1S. VSN44 preparation

Methyl (Z)-(3-(6-(dimethylamino)-6-oxohex-1-en-1-yl)benzoyl)-D-alaninate

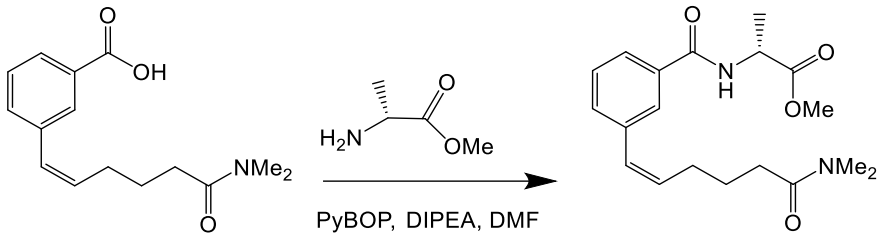

methyl (*Z*)-(3-(6-(dimethylamino)-6-oxohex-1-en-1-yl)benzoyl)-*D*-alaninate

To the substituted benzoic acid (139 mg, 1 mmol) in DMF (1 mL) was added the Ala(OMe) in DMF (1 mL) and the PyBOP (572 mg, 1.1 mmol) added in DMF (2 mL). DIPEA (142 mg, 191 µL, 1.1 mmol) was added dropwise, and the reaction stirred at room temperature overnight. Water (50 mL) was added and ethyl acetate (100 mL). The layers were stirred (5 mins), separated, and the ethyl acetate layer washed with brine (2 x 100 mL), dried (Na_2SO_4) to give the crude product (650 mg). This was flash chromatographed using a 25g Puriflash (silica) column, cyclohexane: acetone 15-45% gradient. Yield 180 mg, 0.54 mmol, 54%.

^{1}H NMR (500 MHz, $CDCl_3$) δ 7.77 (s, 1H), 7.71 (dt, J = 1.6, 7.4, 1H), 7.42 – 7.38 (m, J = 7.4, 1H), 7.38 – 7.31 (m, 2H), 6.46 (d, J = 11.6, 1H), 5.74 (dt, J = 7.7, 11.6, 1H), 4.84 – 4.76 (m, J = 7.2, 1H), 3.77 (s, 3H), 2.95 (s, 3H), 2.90 (s, 3H), 2.42 – 2.30 (m, 4H), 1.83 (p, J = 7.2, 2H), 1.64 (s, 2H), 1.54 (d, J = 7.2, 3H).

^{13}C NMR (126 MHz, $CDCl_3$) δ 173.78, 172.63, 167.13, 137.88, 134.10, 133.23, 132.09, 128.90, 128.53, 127.12, 125.77, 52.54, 48.67, 37.30, 35.54, 32.60, 28.30, 24.99, 18.31, 17.66

(Z)-(3-(6-(dimethylamino)-6-oxohex-1-en-1-yl)benzoyl)-D-alanine

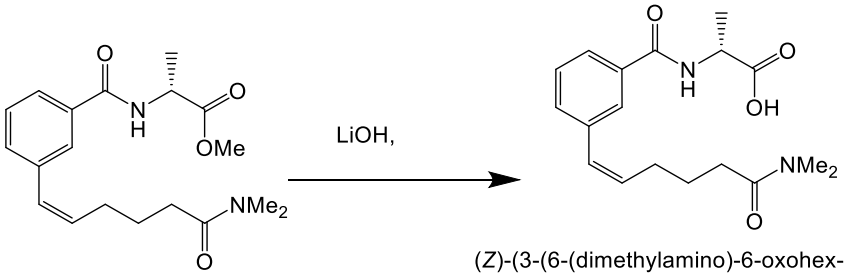

(*Z*)-(3-(6-(dimethylamino)-6-oxohex-1-en-1-yl)benzoyl)-*D*-alanine

The ester (135 mg, 0.41 mmol) in THF (2 mL) was added to lithium hydroxide, hydrate 84 mg, 2 mmol) in water (1 mL). The reaction was stirred at room temperature for 24 hrs. The THF was removed on the rotary evaporator and the residue taken up in 10% aq. Citric acid (10 mL). The aqueous mixture was extracted with DCM (3 x 30 mL) and dried over Na_2SO_4. Crude yield 307 mg. Attempts to purify using flash chromatography were unsuccessful. The product was finally purified by preparative LCMS (C18) using: Solvent A, 5% MeOH/95% H_2O, 0.1% HCOOH. Solvent B, 95% MeOH/5% H_2O, 0.1% HCOOH. Gradient 10% A to 95% over 8 min. The fractions were combined, and the volatiles removed on a rotary evaporator. The final aqueous mixture was freeze dried.

^{1}H NMR (500 MHz, $CDCl_3$) δ 9.03 (s, 1H), 7.74 (s, 1H), 7.73 – 7.67 (m, J = 7.7, 2H), 7.38 – 7.34 (m, 1H), 7.34 – 7.31 (m, 1H), 6.43 (d, J = 11.6, 1H), 5.70 (dt, J = 7.7, 11.6, 1H), 4.80 – 4.70 (m, 1H), 2.96 (s, 3H), 2.89 (s, 3H), 2.35 (t, J = 7.1, 3H), 2.32 – 2.22 (m, 1H), 1.86 – 1.73 (m, 2H), 1.54 (d, J = 7.2, 3H).

^{13}C NMR (126 MHz, $CDCl_3$) δ 175.39, 173.51, 168.12, 137.75, 133.65, 132.95, 132.31, 128.96, 128.62, 127.07, 126.06, 49.28, 37.55, 35.84, 32.64, 28.27, 25.08, 17.84.

FIGURE S1

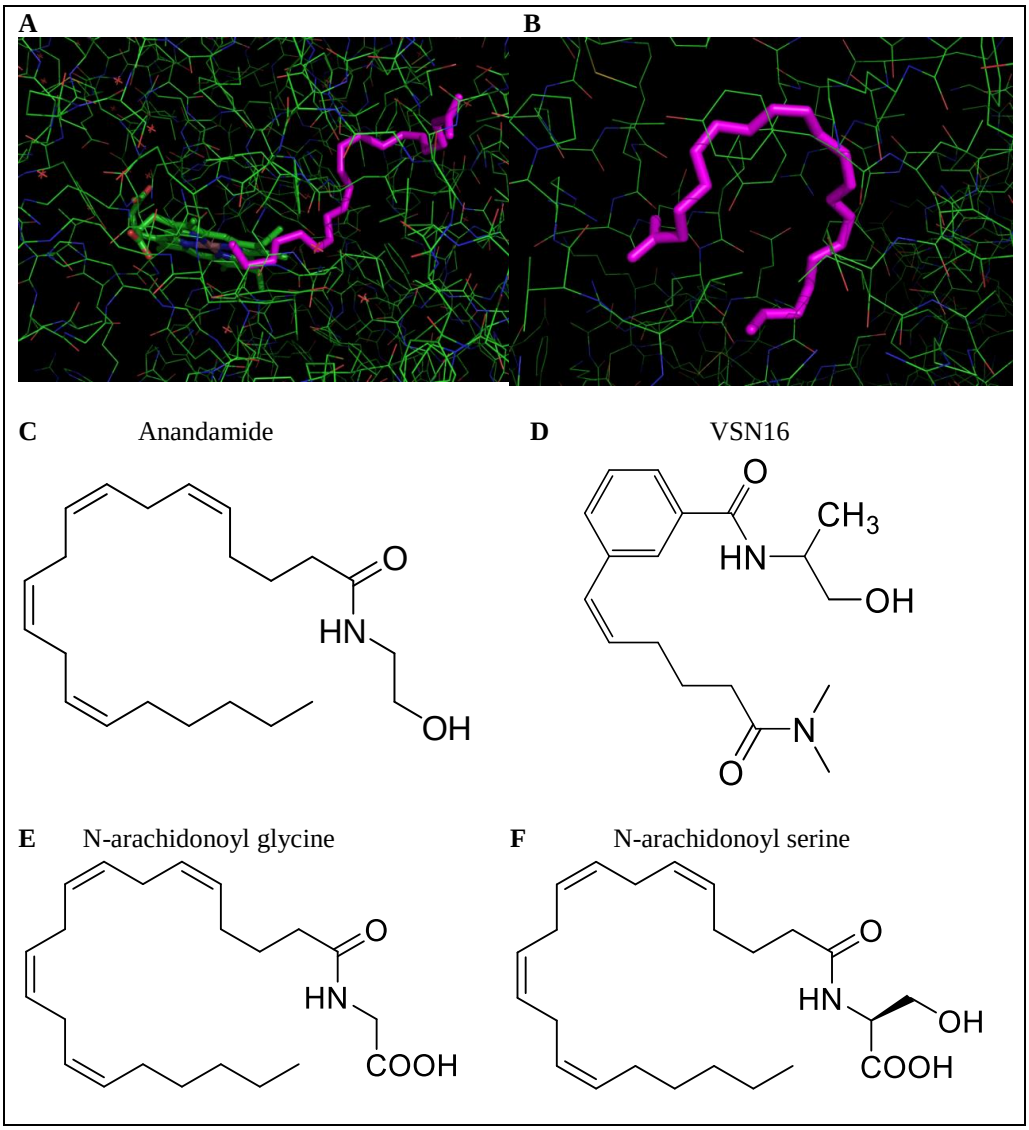

Biological conformations of the arachidonic acid chain. (**A, B**) "C" type conformations of the polyene chain from diverse biological targets from X-ray. This suggested that conformational restriction of (**C**) anandamide would be useful approach to generate novel molecules as in (**D**) VSN16. This has structural similarities with (E) N-arachidonoyl glycine and (F) N-arachidonoyl serine.

FIGURE S2.

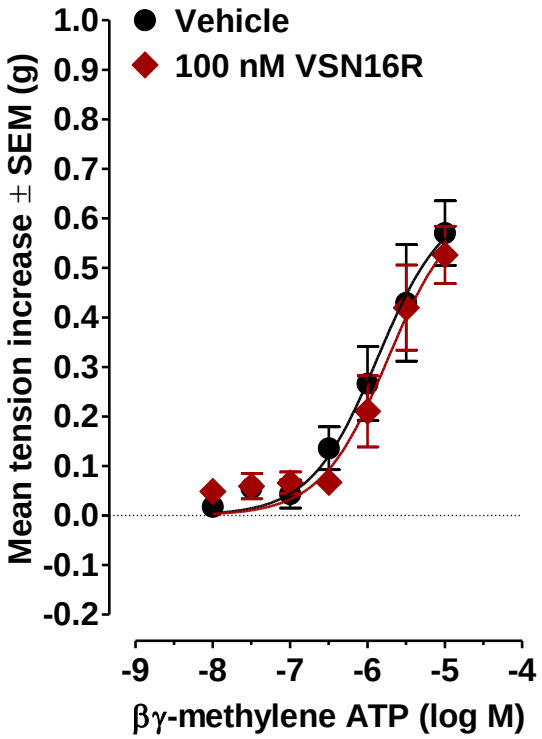

VSN16R does not inhibit beta gamma methylene adenosine triphosphatase-induced muscle contraction in the vas deferens. Mouse vas deferens were treated with either DMSO vehicle or 100 nM VSN16R 30 min before the first organ bath injection of various concentrations of βγ-methylene ATP into the organ bath . The results represent the mean ± SEM of βγ-methylene ATP-induced increases in tension (expressed in grams) of electrically unstimulated vasa deferentia. (n=6/group).

FIGURE S3

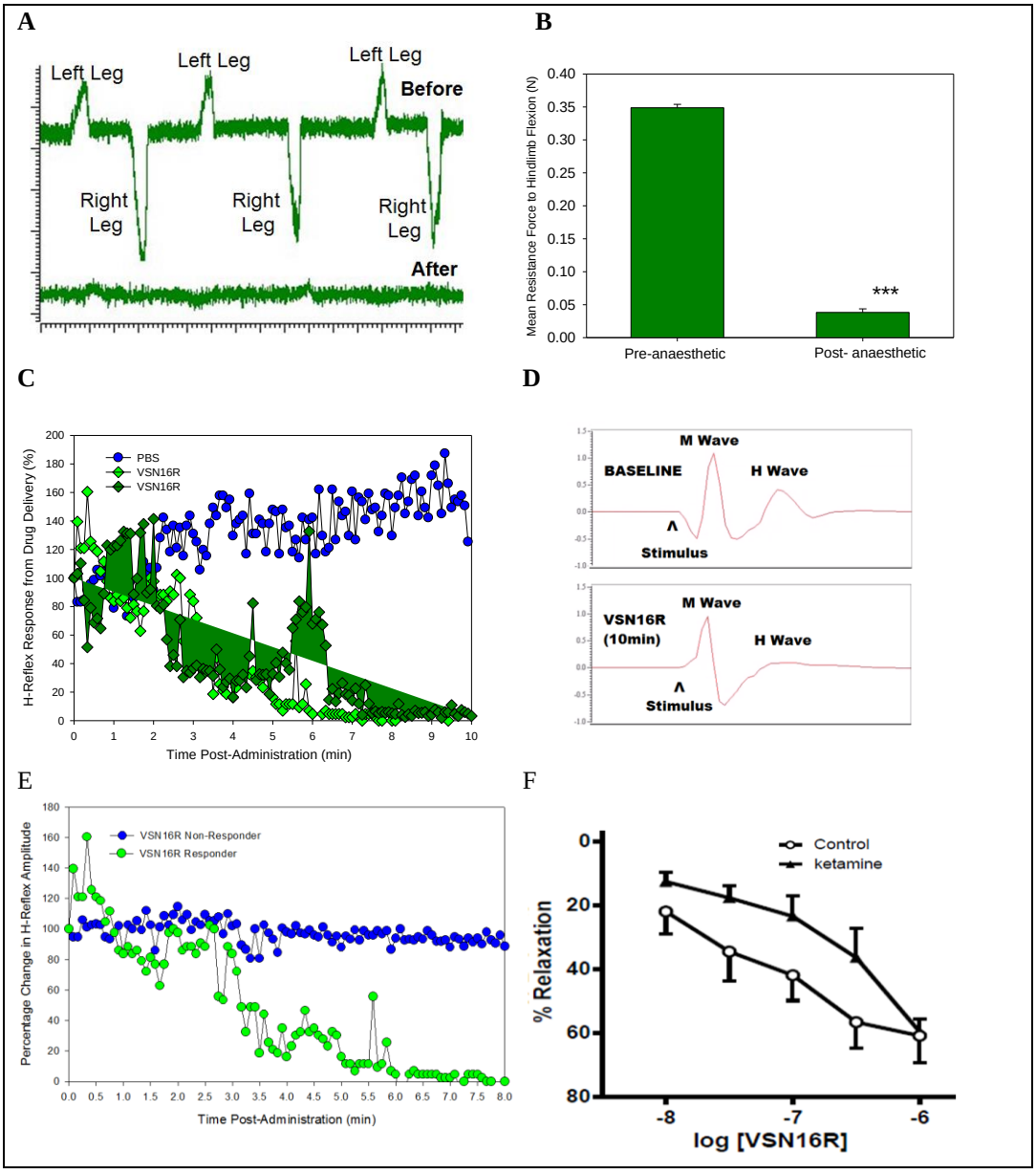

Anaesthetics inhibit spasticity and muscle tone and can interfere with the action of VSN16R.
(**A**) Strain gauge recording before and after (5min) the induction of ketamine and medetomide anesthesia, typically used for rodent electrophysiology studies. (**B**) Loss of muscle tone of spastic animals following anaesthetic showing measurement of resistance to limb flexion before and 5min after anesthesia.*** P<0.001 compared to baseline before anesthetic using paired t test (n=5 animals) (**C**) The magnitude of the H-wave was measured in the shin muscle in spastic animals following sciatic nerve stimulation (100%= H wave at administration of 30mg/kg i.v. VSN16R in phosphate buffered saline at 0min). Although n=0/3 PBS-treated animals showed an inhibition of the H reflex, this could be inhibited by VSN16R (**D**) Electrophysiological trace of the shin muscle following stimulation of a spastic mouse before and after 30mg/kg i.v. VSN16R administration. (E) However, the H reflex was only inhibited in some (3/5) animals responded (Green circles), whereas others did not (blue circles). Trace of individual mice (**F**) However, it was subsequently found that ketamine (200 μM. To represent anaesthetic levels in blood) can inhibit the mechanism of action of VSN16R in part of the dose-response curve to methoxamine-evoked contraction of rat mesenteric artery (n= 5-6 cultures). Ketamine blocks NMDA receptors, that limits calcium ion fluxes that can influence BK_{Ca} function and can inhibit the inside-out current of BK_{Ca} channels with an EC_{50} = ~25μM (Denson DD et al. Brain Res 638:61). In contrast to healthy animals, mice with spasticity did not tolerate anaesthetics, which caused death in some instances, prompting discontinuation of the approach prior to attempted dose reduction.

FIGURE S4

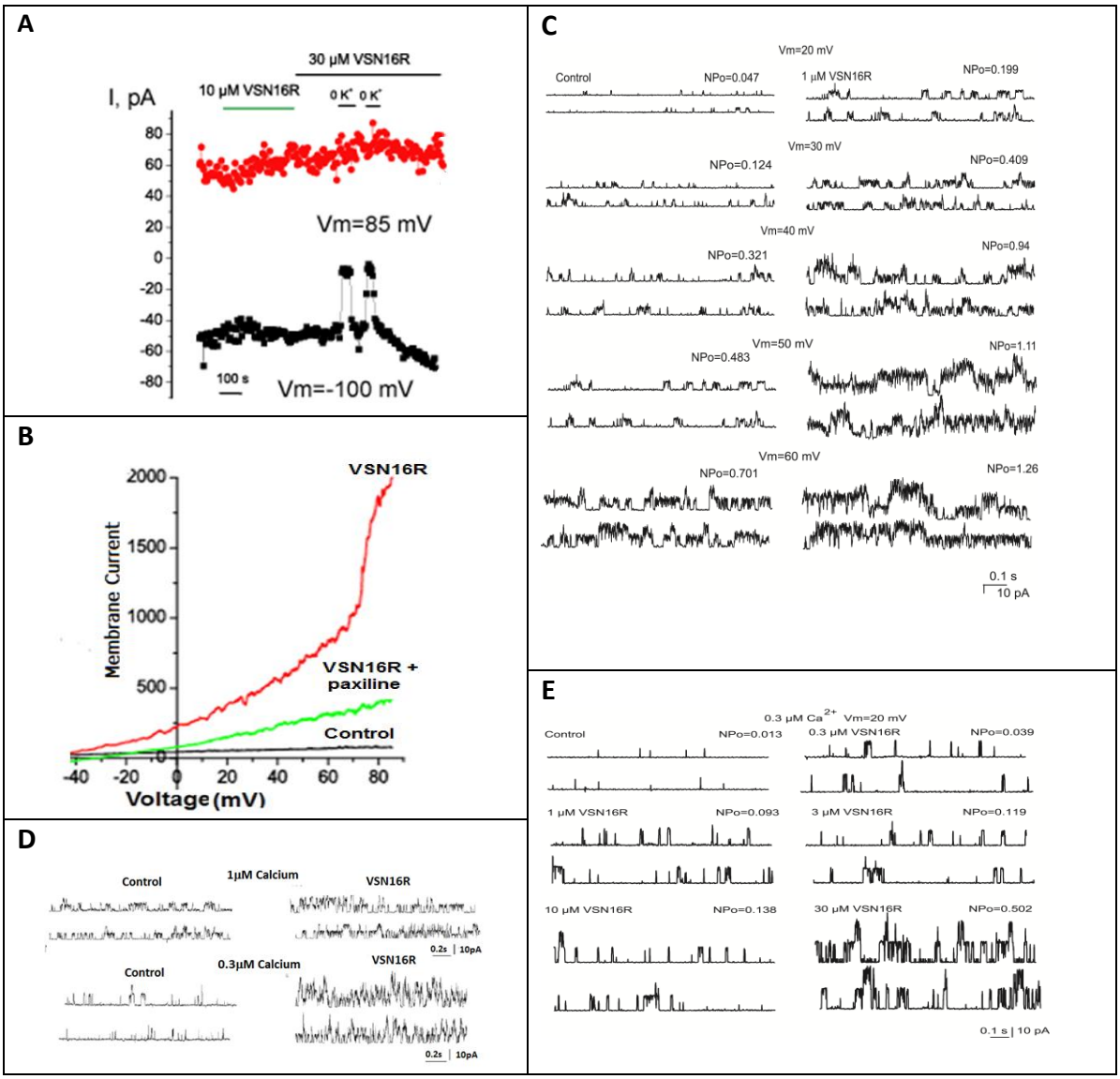

Patch Clamp analysis of VSN16R activity on BK_{Ca} channels. (**A**) Primary pig aorta do not respond to VSN16R (n=3 patches). Time course of the current development at -100 mV (lower) and +85 mV (upper) in response to VSN16R or the removal of potassium. (**B**) Whole cell currents of human EA.hy926 cells in response to voltage ramps before (control), and during exposure to 15µM VSN16R in the absence and presence of 2µM paxilline. The current represents the influence of endogenously expressed conducting ion channels within the cell, but the sensitivity to paxilline indicates that the majority response was mediated by BKca channels. (**C-E**) This was shown in single channel patch clamp experiments in EA.hy926 cells. (**C**) Voltage dependence of activity of VSN16R in inside-out patch clamp of single BK_{Ca} channels VSN16R. (**D**) Calcium dependence of activity of VSN16R. Single BK_{Ca} channel activity in inside-out patch held at +60 mV and exposed to either 1µM or 0.3µM free Ca^{2+} concentrations before (control) and after treatment with 3 µM VSN16R. (**E**) VSN16R exhibits a concentration-dependent induction of potassium currents in inside-out patch clamp of single BK_{Ca} in EA.hy926 cells. The patch was held at 20 mV and exposed to 0.3 µM free Ca^{2+} under symmetrical K^+ conditions. Representative traces that were repeated.

FIGURE S5.

Receptor binding profile of VSN16R

A *Receptors with Negligible Activity following incubation with 10μM VSN16R*

human: A_1, A_{2A}, A_3, α_1(non-selective), α_2(non-selective),β_1, AT_1, BZD, β_2, CCK_A,, CB1, CB2, D1, D2S, ET_A, GABA (non-selective), GAL2, CXCR2, CCR1, H_1, H_2, MC_4, ML_1, M_1, M_2, M_3, NK_2, NK_3, Y_1, Y_2,NT_1,δ_2, κ, μ, ORL1, 5-HT_{1A}, 5-HT_{1B}, 5-HT_{2A}, 5-HT_3, 5-HT_{5A}, 5-HT6, 5-HT_7, sst(non-selective), VIP_1, V_{1a}, Ca^{2+} channel (L verapamil site), K^+_V channel, SK^+Ca channel (KCNN2), Na^+ channel (site 2), Cl^- channel, fatty acid amide hydrolase, monoglycerol lipase, NE transporter, DA transporter, Nav 1.5 Na^+ channel, hERG Kv11.1 K^+ channel (tested to 100 μM), GPR6, GPR12, GPR23, GPR35, GPR55, GPR119, EDG1, EDG2, EDG3, EDG3, EDG4, EDG5, EDG6, EDG7, EDG8, $GABA_A$, $GABA_B$, GlyR , TrK_B, Na^+-Ca^{2+} exchanger.

B *VSN16R does not bind to Cannabinoid Receptors*

Receptor	Activity of VSN16R (Max. Tested)	Positive Control (Affinity and Assay)
CB_1 Receptor (Rat cerebellar membranes)	No Activity (300μM)	CP55,940 (IC_{50} = 0.36nM. Competitive ligand binding)
hCB_1 Receptor (CHO.CNR1)	No Activity (10μM)	CP55,940 (EC_{50} =24nM cAMP Assay)
hCB_1 Receptor (HEK293.CNR1)	No Activity (10μM)	Anandamide (IC_{50} =344nM GTPγS Binding assay)
hCB_2 Receptor (HEK293T.CNR2)	No Activity (10μM)	CP55,940 (EC_{50} =1nM cAMP assay)
hCB_2 Receptor (CHO-K1.CNR2)	No Activity (10μM)	(R)+WIN55,212 (IC_{50} =5.2nM GTPγS Binding assay) CP55,940 (IC_{50} =2.37nM GTPγS Binding assay)
hGPR55 (HEK293.GPR55)	No Activity (10μM)	Lysophosphoinositol (EC_{50} =1.09μM. Ca2+ Ion Flux assay)

C

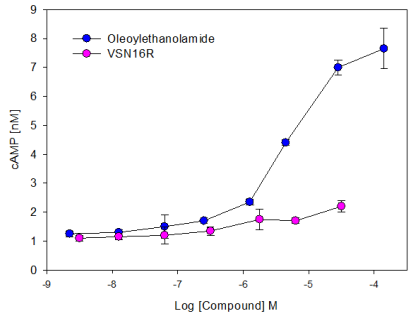

D

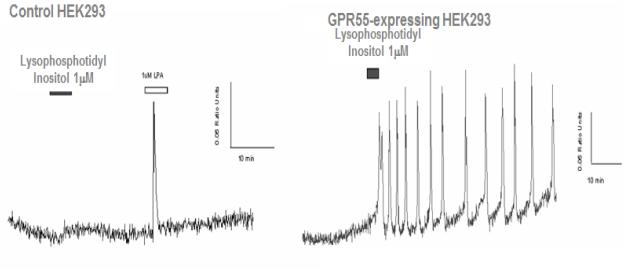

E

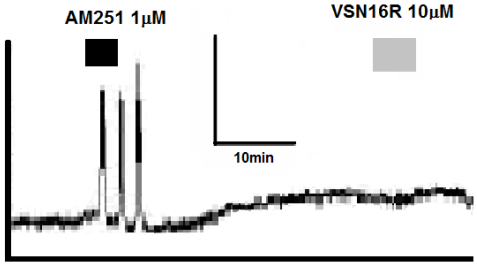

F

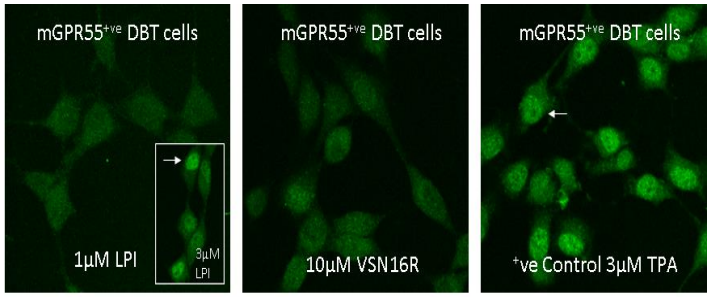

Receptors and other targets that VSN16R fails to bind/activate (**A**) Receptors lacking activity with 10μM VSN16R. Binding assays and positive controls were performed by Cerep, Multispan, DiscoverX, MDS pharma and Chantest. (**B)** Lack of activity of VSN16R on CB_1 and CB_2 cannabinoid receptors (**C**) Relative lack of activity of VSN16R agonism on U20S cells transfected with human GPR119 compared with oleoylethanolamide as assessed using cyclic AMP assay (**D**). HEK293 cells do not respond to lysophosphoinositol (LPI. GPR55 agonist) stimulation, but respond to lysophophatidic acid (LPA), unless they are transfected with human *GPR55* (left) as assessed using calcium ion fluxes (Henstridge CM et al. Br J Pharmacol 2010; 160:604). (**E**) HEK293.*GPR55* demonstrate calcium fluxes following stimulation with AM251 but do not respond to VSN16R (**F**) Lack of activity of VSN16R on DBT cells stably transfected with mouse *Gpr55*. These were incubated with 1-3μM LPI, 10μM VSN16A or the 10μM and the nuclear expression of cAMP response element-binding protein (CREB) was assessed by immunocytochemistry (Henstridge CM et al. 2010).

TABLE S1

VSN16R does not induce neurobehavioural behavioural tests in an Irwin test

Irwin Test Outcomes	Behavioural Effects Unchanged following VSN16R
Behavioural Profile	Alertness, Passivity, Stereotypy, Vocalizations, Transfer Reactivity, Touch, Escape, Tail-Pinch, Toe-Pinch, Pinna Reflex, Corneal Reflex, Startle Response, Visual Placing responses
Neurological profile	Body Elevation, Limb Position, Tail Elevation, Limb Tone, Grip Strength, Body Tone, Abdominal Tone, Change in Gait, Catalepsy, Righting Reflex, Twitches, Convulsion (Clonic, Tonic))
Autonomic profile	(Palpebral Size, Excretion (Urination, Diarrhoea), Secretion (Salivation, Lacrimation), Piloerection, Body Temperature change, Skin Colour (Blanch, Flush, Cyanosis) change, Respiration (Fast, Slow, Deep, Irregular) response changes or Death.

Rats were fed with 120mg/kg p.o. VSN16R in water and behavioural effects in a standard Irwin test (Roux et al. 2005) was assessed. n=5 rats.

TABLE S2

VSN16R does not induce cytochrome P450 enzymes

	IC_{50} Inhibition of substrate binding	
Enzyme	VSN16R	EC_{50} Positive Control
CYP450 1A2	>10μM VSN16R	0.28μM 4-OH-4 androstene 3,17-dione
CYP450 1A2	>10μM VSN16R	0.96μM Furafylline
CYP450 2A6	>10μM VSN16R	0.20μM Tranylcypromine
CYP450 2B6	>10μM VSN16R	2.9μM Ketoconazole
CYP450 2C19	>10μM VSN16R	8.1μM Tranylcypromine
CYP450 2C8	>10μM VSN16R	1.1μM Quercetin
CYP450 2C9	>10μM VSN16R	0.77μM Sulfaphenazole
CYP450 2D6	>30μM VSN16R	0.40μM Quinidine
CYP450 2E1	>10μM VSN16R	8.0μM 4-methylpyrazole
CYP450 3A4	>10μM VSN16R	0.08μM Ketoconazole
CYP450 3A5	>10μM VSN16R	0.36μM Ketoconazole
CYP450 3A7	>10μM VSN16R	0.45μM Ketoconazole

Inhibition of binding of either 3-cyano-7-ethoxycoumarin, dibenzylfluorescein or 7-benzyoxy-4-(trifluoromethyl) coumarin in human enzyme transfected BTI NN-5B1-4 cells or Sf9 insect cells or inhibition of dextromethorphan substrate to CYP450 2D6 in liver microsomes.

TABLE S3.
VSN16R does not induce chromosomal mutagenesis

Strain of Organism	Treatment	Dose	Revertants per plate
First Mutation without Metabolic Stimulation			
TA1535	DMSO	-	12.3 ± 3.1
	VSN16R	17µg	9.0 ± 6.6
		5000µg	13.7 ± 2.1
TA1537	DMSO	-	12.3 ± 4.5
	VSN16R	17µg	13.3 ± 1.5
		5000µg	7.0 ± 1.7
TA98	DMSO	-	18.7 ± 2.3
	VSN16R	17µg	15.3 ± 4.7
		5000µg	18.3 ± 7.1
TA100	DMSO	-	90.0 ± 10.6
	VSN16R	17µg	79.3 ± 7.6
		5000µg	79.3 ± 5.5
WP2uvvA	DMSO	-	4.3 ± 2.1
	VSN16R	17µg	5.3 ± 0.6
		5000µg	1.3 ± 1.2
Second Mutation without Metabolic Stimulation			
TA1535	DMSO	**-**	9.0 ± 5.61
	VSN16R	17µg	14.0 ± 5.6
		5000µg	11.3 ± 3.5
TA1537	DMSO	-	8.7 ± 3.1
	VSN16R	17µg	12.3 ± 2.9
		5000µg	10.3 ± 2.9
TA98	DMSO	-	25.7 ± 8.3
	VSN16R	17µg	23.3 ± 1.2
		5000µg	23.7 ± 1.2
TA100	DMSO	-	79.5 ± 4.9
	VSN16R	17µg	85.7 ± 6.7
		5000µg	99.3 ± 5.5
WP2uvvA	DMSO	-	6.7 ± 1.2
	VSN16R	17µg	10.3 ± 6.7
		5000µg	8.0 ± 4.6

VSN16R was incubated at various concentrations with either TA1535, TA1537, TA98 and TA100 strains of *Salmonella typhimurium*, which carry mutations in genes involved in histidine synthesis, and WP2uvvA *Escherichia coli*. The bacteria are spread on agar plates with limiting histidine content and incubated for 48 h. The number of histidine gene negative to positive revertants was assessed in two experiments. The results represent the mean ± SD. n=3/group. This was performed by Charles Rivers, Ltd, UK.

TABLE S4.
VSN16R does not induce tissue toxicology of VSN16R in rats and dogs

Tissue Analysed	Result of Tissue Analysis in Rats	Result of Tissue Analysis in Dogs
Artery, Aorta	Negative	Negative
Bone Marrow femur	Negative	Negative
Bone Marrow sternum	Negative	Negative
Bone, Sternum	Negative	Negative
Bone, Sternum	Negative	Negative
Brain	Negative	Negative
Cervix	Negative	Negative
Epididymus	Negative	Negative
Eye	Negative	Negative
Adrenal Gland	Negative	Negative
Mammary Grand	Negative	Negative
Parathyroid Gland	Negative	Negative
Pituitary Gland	Negative	Negative
Prostate Gland	Negative	Negative
Salivary Gland	Negative	Negative
Seminal Vesicle Gland	Negative	Negative
Gut associated lymphoid	Negative	Negative
tissue	Negative	Negative
Kidney	Negative	Negative
Heart	Negative	Negative
Large Intestine caecum	Negative	Negative
Large Intestine colon	Negative	Negative
Large Intestine rectum	Negative	Negative
Liver	Centrilobular hypertrophy *	Negative
Lung	Negative	Negative
Mandibular Lymph Node	Negative	Negative
Mesenteric Lymph Node	Negative	Negative
Skeletal Muscle	Negative	Negative
Nasal Cavity	Negative	Negative
Sciatic Nerve	Negative	Negative
Oesophagus	Negative	Negative
Ovary	Negative	Negative
Pancreas	Negative	Negative
Skin	Negative	Negative
Small Intestine, duodenum	Negative	Negative
Small Intestine, Ileum	Negative	Negative
Small Intestine, Jejunum	Negative	Negative
Spinal Cord	Negative	Negative
Spleen	Negative	Negative
Stomach	Negative	Negative
Testis	Negative	Negative
Thymus	Negative	Negative
Tongue	Negative	Negative
Trachea	Negative	Negative
Ureter	Negative	Negative
Urinary bladder	Negative	Negative
Uterus	Negative	Negative
Vagina	Negative	Negative

Following 28 day toxicology of feeding either: rats treated with 100mg/kg, 300mg/kg, 1000mg/kg p.o. (n-20/group) or dogs treated with 50mg/kg, 100mg/kg or 200mg/kg p.o. (n=6/group). Tissues were collected fixed in formalin, embedded in paraffin-wax sectioned and stained with hematoxylin and eosin and examined by a veterinary pathologist for evidence of toxicity. There was generally no microscopic findings attributed to treatment with VSN16R. Studies were performed by Charles Rivers, Ltd. However, * There was hypertrophy of the liver that was evident at high doses VSN16R was associated with liver weight (mean ± SD) increases: 11.0 ± 1.2g placebo, 11.6 ± 1.3g (300mg/kg p.o.), 16.7 ± 2.1g (1000mg/kg p.o. $P<0.001$ assessed using Students t test. n= 10 female rats/group) associated with liver enzyme induction, supporting enhanced VSN16R clearance in pharmacokinetic studies. This was not seen in dogs or doses below 300mg/kg in rats.

TABLE S5.
Lack of hypotension induced by VSN16R in dogs

Parameter	Time	Vehicle	50mg/kg	100mg/kg	200mg/kg
Heart Rate (bpm)	0 min	105 ± 9	104 ± 9	107 ± 9	101 ± 9
	30min	97 ± 9	104 ± 9	114 ± 9	125 ± 9
	60min	121 ± 9	119 ± 9	111 ± 9	134 ± 9
Arterial Pressure (mm Hg)	0 min	105 ± 9	102 ± 5	105 ± 5	105 ± 5
	30min	94 ± 5	97 ± 5	99 ± 5	97 ± 5
	60min	112 ± 5	106 ± 5	106 ± 5	102 ± 5
Systolic Blood Pressure (mm Hg)	0 min	136 ± 6	139 ± 6	142 ± 6	141 ± 6
	30min	130 ± 6	141 ± 6	139 ± 6	130 ± 6
	60min	151± 6	143 ± 6	138 ± 6	130 ± 6
Diastolic Blood Pressure (mm Hg)	0 min	79 ± 4	83 ± 4	86 ± 4	87 ± 1
	30min	77 ± 4	83 ± 4	86 ± 4	87 ± 1
	60min	92 ± 4	87 ± 4	91 ± 4	88 ± 4

Adult male Beagle dogs implanted previously with a DSI Physio Tel TL11-M2 D70-PCT intramuscular telemetry device received either: 50mg/kg, 100mg/kg or 200mg/kg p.o. VSN16R in water or water. The results represent the mean ± SD. n=4.

TABLE S6.
Demographics of humans in phase I double-blind, placebo-controlled trial

Dosing Dose Food	Single 25mg Fasted	Single 50mg Fasted	Single 100mg Fasted	Single 200mg Fasted	Single 200mg Fed	Single 400mg Fasted	Single 800mg Fasted	Single VSN16R Total	Single Placebo Total
Males/Total	6/6	6/6	6/6	6/6	6/6	6/6	6/6	42/42	1414
Age (Years)	34 ± 9	31 ± 9	30 ± 7	35 ± 8	36 ± 10	29 ± 6	36 ± 9	33 ± 8	31 ± 7
Weight (Kg)	81 ±9	81 ±9	86 ± 6	82 ± 12	82 ± 10	76 ± 6	80 ± 9	81 ± 9	81 ±13
BMI (Kg/m^2)	26 ± 3	25 ± 2	26 ± 2	25 ± 4	27 ± 3	26 ± 2	26 ± 2	26 ± 3	26 ± 3

Dosing Dose Food	b.i.d. 25mg Fasted	b.i.d 100mg Fasted	b.i.d 400mg Fasted	b.i.d VSN16R Total	b.i.d Placebo Total
Males/Total	6/6	6/6	6/6	18/18	6/6
Age (Years)	35 ± 7	32 ± 10	31 ± 8	32 ± 8	32 ± 9
Weight (Kg)	80 ± 8	77 ± 9	68 ± 6	75 ± 9	80 ± 13
BMI (Kg/m^2)	25 ± 3	25 ± 2	22 ± 3	24 ± 3	26 ± 2

The results represent the mean ± SD. VSN16R was administered a single dose or twice daily (b.i.d.) for 7 days.

TABLE S7. *Single Dose of VSN16R did not affect haematology and blood chemistry in humans*

Outcome	Time	Placebo	25mg	800mg
Haematology				
Hematocrit	Day -1	0.412 ± 0.026	0.417 ± 0.015	0.423 ± 0.024
	Day 2	0.416 ± 0.021	0.425 ± 0.021	0.421 ± 0.016
Haemoglobin	Day -1	8.9 ± 0.5	9.4 ± 0.4	9.0 ± 0.6
(mmol/L)	Day 2	9.0 ± 0.5	9.4 ± 0.5	9.3 ± 0.5
Red Blood Cells	Day -1	5.01 ± 0.58	4.90 ± 0.28	4.84 ± 0.36
(10^{12} cells/L)	Day 2	5.07 ± 0.57	4.94 ± 0.30	4.87 ± 0.30
White Blood Cells	Day -1	6.2 ± 1.0	4.9 ± 1.4	5.6 ± 1.3
(10^9 cells/L)	Day 2	5.7 ± 0.9	5.2 ± 1.2	5.0 ± 1.1
Lymphocytes	Day -1	2.1 ± 0.3	1.9 ± 1.0	1.8 ± 0.5
(10^9 cells/L)	Day 2	1.6 ± 0.2	1.9 ± 0.6	1.8 ± 0.6
Monocytes	Day -1	0.6 ± 0.1	0.6 ± 0.2	0.5 ± 0.1
(10^9 cells/L)	Day 2	0.6 ± 0.1	0.5 ± 0.1	0.5 ± 0.1
Neutrophils	Day -1	3.4 ± 0.7	2.4 ± 0.7	2.5 ± 1.1
(10^9 cells/L)	Day 2	3.1 ± 0.4	2.5 ± 0.6	2.7 ± 1.2
Eosinophils	Day -1	0.2 ± 0.1	0.1 ± 0.1	0.3 ± 0.2
(10^9 cells/L)	Day 2	0.2 ± 0.2	0.2 ± 0.1	0.3 ± 0.1
Basophils	Day -1	0.0 ± 0.0	0.0 ± 0.0	0.0 ± 0.0
(10^9 cells/L)	Day 2	0.0 ± 0.1	0.0 ± 0.0	0.0 ± 0.0
Serum Chemistry				
Bilirubin	Day -1	10.8 ± 4.3	12.5 ± 5.3	9.9 ± 2.2
(µmol/L)	Day 2	14.1 ± 4.1	14.9 ± 6.1	11.4 ± 3.0
Phosphate	Day -1	1.19 ± 0.16	1.18 ± 0.18	1.30 ± 0.18
(mmol/L)	Day 2	1.13 ± 0.10	1.20 ± 0.10	1.02 ± 0.10
Potassium	Day -1	4.32 ± 0.32	4.17 ± 0.30	4.34 ± 0.28
(mmol/L)	Day 2	4.29 ± 0.26	4.27 ± 0.18	4.19 ± 0.25
Sodium	Day -1	143 ± 2	141 ± 2	143 ± 2
(mmol/L)	Day 2	142 ± 2	141 ± 2	142 ± 3
Chloride	Day -1	103 ± 2	104 ± 2	102 ± 3
(mmol/L)	Day 2	103 ± 1	104 ± 2	104 ± 1
Magnesium	Day -1	0.8 ± 0.1	0.8 ± 0.0	0.8 ± 0.1
(mmol/L)	Day 2	0.8 ± 0.1	0.8 ± 0.0	0.8 ± 0.1
Calcium	Day -1	2.39 ± 0.10	2.37 ± 0.09	2.36 ± 0.06
(mmol/L)	Day 2	2.36 ± 0.08	2.40 ± 0.08	2.35 ± 0.04
Urea	Day -1	4.8 ± 0.7	5.5 ± 1.0	5.0 ± 1.1
(mmol/L)	Day 2	4.7 ± 0.7	4.4 ± 0.9	4.7 ± 0.4
Amylase	Day -1	65 ± 17	66 ± 21	55 ± 12
(U/L)	Day 2	59 ± 15	65 ± 21	50 ± 12
Albumin	Day -1	44 ± 2	42 ± 1	42 ± 1
(g/L)	Day 2	42 ± 3	42 ± 1	42 ± 1
Globulin	Day -1	29.4 ± 2.5	28.8 ± 5.6	29.4 ± 2.2
(g/L)	Day 2	29.5 ± 3.7	28.8 ± 5.6	28.9 ± 1.2
Creatinine	Day -1	79 ± 9	85 ± 14	85 ± 14
(µmol/L)	Day 2	78 ± 11	84 ± 10	84 ± 10
Glucose	Day -1	4.55 ± 0.64	4.78 ± 0.46	4.45± 0.32
(mmol/L)	Day 2	5.06 ± 1.11	4.78 ± 0.58	5.51 ± 0.92
Triglycerides	Day -1	1.47 ± 0.68	0.85 ± 0.36	1.28 ± 0.71
(mmol/L)	Day 2	1.41 ± 0.49	1.26 ± 0.25	1.55 ± 0.61
Cholesterol	Day -1	4.57 ± 0.97	4.71 ± 0.75	4.63 ± 0.94
(mmol/L)	Day 2	4.65 ± 0.65	4.79 ± 0.77	4.68 ± 0.78
Urea	Day -1	4.8 ± 0.7	5.5 ± 1.0	5.0 ± 1.1
(mmol/L)	Day 2	4.7 ± 0.7	4.4 ± 0.9	4.7 ± 0.4

Adult males were received gelatin capsules containing placebo (n=14) or 25mg (n=6) or 800mg (n=6 humans/group) VSN16R. Plasma was collected before and after drug administration. The results represent the mean ± SD.

TABLE S8. *Single dose of VSN16R did not affect coagulation, urinanalysis, vital signs and electrocardiograms in humans*

Outcome	Time	Placebo	25mg	800mg
Coagulation				
Partial Prothrombin Time	Day -1	10.6 ± 0.5	10.5 ± 0.1	10.5 ± 0.4
(s)	Day 2	10.8 ± 0.5	10.8 ± 0.3	10.9 ± 0.5
Thrombin Time	Day -1	15.7 ± 0.8	16.1 ± 0.8	15.9 ± 1.2
(s)	Day 2	16.0 ± 1.0	16.2 ± 0.8	15.9 ± 1.2
Activated Partial Thrombin	Day -1	26.4 ± 1.0	26.4 ± 1.0	25.4 ± 1.5
Time (s)	Day 2	26.4 ± 0.9	26.4 ± 0.9	24.9 ± 1.9
Urinanalysis				
pH	Day -1	6.4 ± 0.8	6.3 ± 0.3	6.1 ± 0.8
	Day 2	6.4 ± 0.7	7.0 ± 0.6	6.0 ± 0.4
Specific Gravity	Day -1	1.018 ± 0.008	1.018 ± 0.010	1.018 ± 0.005
	Day 2	1.019 ± 0.006	1.016 ± 0.012	1.017 ± 0.009
Urine Glucose	Day -1	0.0 ± 0.0	0.0 ± 0.0	0.0 ± 0.0
(mmol/L)	Day 2	0.0 ± 0.0	0.0 ± 0.0	0.0 ± 0.0
Ketones	Day -1	0.0 ± 0.0	0.0 ± 0.0	0.0 ± 0.0
(mmol/L)	Day 2	0.0 ± 0.0	0.0 ± 0.0	0.0 ± 0.0
Urine RBC	Day -1	0.0 ± 0.1	0.0 ± 0.0	0.0 ± 0.0
(mg/L)	Day 2	0.0 ± 0.0	0.0 ± 0.0	0.0 ± 0.0
Urine Protein	Day -1	0.05± 0.04	0.10 ± 0.13	0.04 ± 0.04
(g/L)	Day 2	0.07 ± 0.09	0.08 ± 0.10	0.06 ± 0.08
Urine Bilirubin	Day -1	0.0 ± 0.0	0.0 ± 0.0	0.0 ± 0.0
(µmol/L)	Day 2	0.0 ± 0.0	0.0 ± 0.0	0.0 ± 0.0
Vital Signs				
Supine Respiratory Rate	Day -1	15 ± 2	14 ± 2	14 ± 2
(Breath/min)	Day 2	15 ± 2	14 ± 2	16 ± 2
Supine Temperature	Day -1	36.6 ± 0.3	36.7 ± 0.3	36.6 ± 0.2
(°C)	Day 2	36.7 ± 0.2	36.6 ± 0.2	36.6 ± 0.2
Supine Systolic Blood	Day -1	120 ± 7	115 ± 9	117 ± 10
Pressure (mmHg)	Day 2	116 ± 9	117 ± 9	118 ± 10
Supine Diastolic Blood	Day -1	67 ± 6	67 ± 10	70 ± 10
Pressure (mmHg)	Day 2	64 ± 8	65 ± 4	71 ± 9
Supine Pulse Rate	Day -1	65 ± 13	60 ± 13	56 ± 7
(beats per min)	Day 2	66 ± 15	61 ± 15	65 ± 9
Electrocardiograms				
Heart Rate	Day -1	60 ± 11	58 ± 10	59 ± 7
(beats per min)	Day 1	61 ± 11	59 ± 12	67 ± 8
PR Duration	Day -1	167 ± 30	189 ± 18	172 ± 20
(msec)	Day 1	165 ± 27	184 ± 20	164 ± 16
QRS Duration	Day -1	101 ± 7	99 ± 8	97 ± 5
(msec)	Day 1	101 ± 9	98 ± 9	98 ± 7
RR Duration	Day -1	1026 ± 228	1061 ± 193	1030 ± 107
(msec)	Day 1	1013 ± 149	1044 ± 185	903 ± 122
QT Duration	Day -1	393 ± 29	399 ± 26	403 ± 21
(msec)	Day 1	391 ± 25	388 ± 26	383 ± 19

Adult males were received gelatin capsules containing placebo (n=14) or 25mg (n=6) or 800mg (n=6 humans/group) VSN16R. The results represent the mean ± SD. Plasma samples were taken before and after dosing. 12-lead electrocardiograms using a Mortara machine and each lead was recorded for at least 3 beats at a speed of 25 mm/s and recorded.

TABLE S9. *Lack of hypotension induced by VSN16R in humans*

Parameter	Time	Placebo	25mg	800mg
Heart Rate (bpm)	0 min	57 ± 12	54 ± 9	63 ± 12
Supine	30min	59 ± 10	55 ± 10	57 ± 6
	60min	57 ± 10	54 ± 9	59 ± 6
Systolic Blood Pressure (mm Hg)	0 min	115 ± 8	116 ± 8	115 ± 9
Supine	30min	114 ± 6	115 ± 7	115 ±9
	60min	114 ± 8	114 ± 5	117 ± 7
Diastolic Blood Pressure (mm Hg)	0 min	66 ± 8	66 ± 7	72 ± 13
Supine	30min	66 ± 7	65 ± 5	68 ± 14
	60min	64 ± 6	63 ± 6	72 ± 8
Heart Rate (bpm)	0 min	79 ± 15	73 ± 9	76 ± 22
Standing	30min	75 ± 12	72 ± 8	81 ± 10
	60min	80 ± 11	75 ± 9	84 ± 11
Systolic Blood Pressure (mm Hg)	0 min	121 ± 9	121 ± 16	123 ± 8
Standing	30min	118 ± 10	120 ± 6	120 ± 6
	60min	117 ± 9	119 ± 8	120 ± 8
Diastolic Blood Pressure (mm Hg)	0 min	78 ± 6	74 ± 6	76± 10
Standing	30min	72 ± 11	75 ± 6	80 ± 9
	60min	73 ± 7	75 ± 7	81 ± 10

Adult males were received gelatin capsules containing placebo (n=14) or 25mg (n=6) or 800mg (n=6) VSN16R. The results represent the mean ± SD. Pulse rate and blood pressure was measured after laying down for 10 min or standing.